Performance Analysis of a Full-Duplex MIMO Decode-and-Forward Relay System With Self-Energy Recycling

MOHD HAMZA NAIM SHAIKH, (Member, IEEE),
VIVEK ASHOK BOHARA, (Senior Member, IEEE), AND ANAND SRIVASTAVA, (Member, IEEE)
Department of Electronics and Communication Engineering, Indraprastha Institute of Information Technology Delhi (IIIT-Delhi), New Delhi 110020, India

Corresponding author: Mohd Hamza Naim Shaikh (hamzan@iiitd.ac.in)

ABSTRACT This paper analyzes the performance of the full-duplex (FD) multiple-input-multiple-output (MIMO) decode-and-forward (DF) relay system in the presence of self-energy recycling (S-ER). Specifically, this work proposes an antenna allocation scheme for S-ER as well as analytically evaluates the performance of this proposed scheme in terms of spectral efficiency (SE), energy efficiency (EE), outage and symbol error rate (SER). Since, the self-interference (SI) is a major bottleneck in achieving the true potentials of FD communication, this work considers SI as an energy harvesting opportunity to enhance the EE of the system. The proposed analysis shows that reserving few antennas for S-ER at the FD-MIMO relay improves the EE, however, it reduces the antenna array gain at the relay for information transmission and reception. Thus, a slight degradation in the SE, outage and SER is observed. Further, an adaptive S-ER technique has been proposed which utilizes the antennas corresponding to the least channel gain with respect to information transmission and reception for S-ER. This adaptive S-ER technique improves the EE and also compensates for the slight degradation in the SE, outage and SER through adaptive antenna allocation. Closed-form expressions for the SE, EE, outage and symbol error rate have been derived for these S-ER techniques. In the end, simulations results are provided to validate the efficacy of the theoretical derivations.

INDEX TERMS Energy efficiency, full-duplex, self-energy recycling, outage, spectral efficiency, self-interference, symbol error rate, antenna allocation, transmit antenna selection, decode-and-forward relaying, multiple-input multiple-output.

I. INTRODUCTION

The tremendous growth and ubiquitous access to wireless services have lead to a manifold increase in the mobile broadband data traffic volume over the last couple of decades [1]. This growing data traffic has also heightened the energy requirement of the wireless networks. As per the estimate suggested in [2], 1500 terawatt-hours of electricity is consumed by the global information communication technology (ICT) ecosystem, which accounts for nearly one-tenth of the total generated electricity. Compounding the problem further is the advent of the fifth-generation (5G) standards that are envisioned to serve an unprecedented large number of devices comprising of sensors, drones, autonomous vehicles,

connected machines, massive internet-of-thing (IoT), etc., providing ubiquitous coverage along with diversified quality-of-service (QoS) requirements [3].

Additionally, the deployment of next-generation wireless networks may also lead to severe environmental and economic concerns. Environmental concerns are mainly related to the harmful impact of the gaseous discharge in the atmosphere due to the consumption of fossil-fuel based energy sources. Presently, ICT systems are accountable for around 5% of the world's CO_2 emissions [4], and this would increase rapidly with the number of connected devices. The economic concerns are also fueled by the escalating costs in operating the wireless network due to the enormous amount of energy consumption. Hence, for sustainable capacity growth, one of the ambitious goals for the 5G systems is to scale down the energy requirements up to 100 times [3]. The overall

The associate editor coordinating the review of this manuscript and approving it for publication was Yasar Amin.

goal is to shift the paradigm towards a green and sustainable wireless standard, which supports an increase in the capacity without adversely impacting the environment and energy consumption.

Various approaches based on resource allocation, hardware architectures, and energy preservation has been proposed in the literature for economizing the energy consumption of a wireless network [5]–[7]. Recently, energy harvesting (EH) techniques have also been proposed wherein the communication system is operated through harvested energy, harnessed through ambient power sources such as solar and wind [8]. Through energy harvesting, a 20% reduction in CO_2 discharge has been estimated in a small cell network [9]. Recently, EH through radio frequency (RF) has gained considerable interest and is increasingly being studied in the context of wireless networks [10]. For instance, the authors in [11] have conducted a comprehensive study on the feasibility and challenges in the deployment of energy harvesting based small cell networks. Further, [12] also summarizes major recent work done in the domain of wireless energy harvesting. The backup provided through RF-EH has been shown to prolong the battery life, thus making their operation sustainable in the long term [12]. Apart from the above, [13]–[16] comprehensively survey various techniques for energy-efficient wireless systems.

Relaying techniques have gained considerable attraction over the past decade for their ability to extend connectivity and network coverage area along with providing higher capacity and better energy efficiency. In a dual-hop network, source and destination are connected through an intermediate node acting as a relay. In conventional relaying networks, two orthogonal channels are required for effective communication. Usually, time-division duplexing or frequency-division duplexing is utilized to provide out-of-band full-duplex (FD) operations. However, this results in a significant loss of precious spectral resources. Utilizing the same time-frequency resource for concurrent transmission and reception, i.e., in-band FD transmission, can theoretically double the SE of the half-duplex (HD) systems [17]. FD relay-based systems have been widely studied in literature [18]–[22]. In [18], a FD amplify-and-forward (AF) relay system is optimized for minimizing symbol error rate (SER) in terms of power allocation and relay location. Further in [19], authors have optimized power allocation and relay position for the FD decode-and-forward (DF) relay system for minimizing the outage probability. An optimal relay selection scheme for a multi-relay scenario has been considered in [20], where the relay selection is optimized for maximizing the signal-to-interference and noise ratio (SINR) in a two-way FD relay network. A multi-hop FD relay-based system is analyzed in [21], where the authors have evaluated the number of FD relays corresponding to the minimum outage. A novel two-timeslot two-way FD relaying has been proposed in [22], where the authors have evaluated the rate and outage performance of the access and backhaul links served by a FD relay.

However, in FD systems, the receiver suffers from strong interference from the transmitter, as it is co-located with the transmitter within the transceiver. Thus, managing this strong self-interference (SI) is a significant challenge in achieving the true potentials of FD systems. Extensive work has been reported in the literature for suppressing SI [23]–[26]. These techniques consist of passive, active RF and analog suppression techniques, which are followed by digital cancellation schemes. As a first step, passive techniques like antenna separation, isolation, etc., mitigate a significant part of SI [23]. Subsequently, passive techniques are generally followed by active RF and analog cancellation [24]. The leftover SI is alleviated through a digital cancellation scheme [25]. Linking multiple-input-multiple-output (MIMO) techniques along with FD relaying system improves the error performance of the system and provides higher capacity through multi-antenna array gain [27]. Further, multiple antennas provide additional suppression of SI through beam-forming techniques [28]. The potential benefits, feasibility and challenges of massive MIMO based in-band full-duplex cellular system has been explored in [29]. Due to the presence of inherent non-idealities in the transmit RF chain, there is some leftover SI even after the digital cancellation, which is termed as residual SI (RSI) [30], [31]. The impact of RSI on the error and diversity performances of a FD AF relay system has been investigated in [30]. Further, in [31], authors have proposed an optimal power allocation scheme for maximizing the capacity of a AF based FD relay system under the impact of RSI.

A. RELATED WORK

Recently, SI has also been explored for energy harvesting in the FD systems [32]–[35]. This is referred to as self-energy recycling (S-ER) [36]. S-ER recycles a part of the transmitted signal energy, which would otherwise be discarded. S-ER based FD relay systems have been studied in [32] for efficient energy transfer and relay of information. Joint transmission in uplink and downlink for a S-ER based FD system has been investigated in [33] for power allocation and data transmission. The impact of time split parameter on the EE of the S-ER based FD downlink system has been studied in [34]. Further [35] discusses a quality-of-service aware beam-forming design in S-ER based FD relay system.

Since RF waves are capable of transmitting information as well as transferring energy, simultaneous wireless information and power transfer (SWIPT) protocol, which combines power transfer and information transmission, have also been recently investigated. The fundamental trade-off between energy and information transmission with respect to SWIPT has been explored in the seminal work of [37]. In [38], authors have discussed the application of SWIPT in improving the EE and the trade-offs between the performance and system complexity. Several works have been reported in the literature that analyzed the performance of SWIPT based FD relay system [39]–[41]. Specifically, [39] proposed optimal and sub-optimal solutions for maximizing throughput in a

MIMO-FD relay system employing a time-switching protocol for energy transfer to the relay. In [40], authors studied the performance of wireless powered dual-hop AF relaying systems and the impact of channel state information and antenna correlations on system performance. A SWIPT based FD system has been analyzed in [41], where the authors have evaluated throughput performance considering both the AF and DF relaying protocol.

As evident from above, there is a considerable amount of literature available on the impact of S-ER in a FD systems, however, to the best of our knowledge, the stand-alone impact of S-ER on a MIMO relay-based FD system has not been investigated yet. Further, most of the prior work on FD wireless energy transfer considers the impact of S-ER assuming a dedicated wireless power transfer from the source.

B. MOTIVATION AND CONTRIBUTIONS

Inspired by the current research in harnessing S-ER, in this paper, we investigate the impact of S-ER on the performance of a FD-MIMO-DF relay system. The proposed analysis considers a multi-antenna based FD relay system where the FD relay is facilitating the transfer of information between a single antenna source and destination. The proposed scenario suits well for a typical wireless cellular architecture, wherein the multi-antenna base station (BS) works as a relay facilitating the exchange of information among the user equipments (UEs). In general, the UEs are constrained by form-factor and complexity issues, so the half-duplex mode is preferred for UEs. Further, it is assumed that BS has enough computational as well as hardware resources to support FD operations. The multiple antennas at the FD relay have also been utilized for S-ER, along with information transmission and reception. It has been shown that allocating more antennas for S-ER increases the EE by contributing more towards EH and reduced circuit power consumption. However, this also reduces the antenna array gain, which adversely impacts the SE, outage and SER performance of the system. The impact of S-ER on the SE, EE, outage and SER in the FD-MIMO-DF relay-based system are studied in this work.

The major contributions of the proposed work are four-fold:

- The performance of a FD-MIMO-DF relay system in the presence of S-ER has been investigated. It has been shown that the system performance is dictated by the source-to-FD relay link since the SI impacts the source-to-FD relay link, whereas the relay-to-destination link is interference-free. Hence, the antennas at the transmit-end of the FD relay can easily be utilized for S-ER, which improves the EE of the system.
- It has been shown that S-ER improves the EE of the system, but it also slightly degrades the SE, outage and SER performance. Further, an adaptive S-ER scheme is proposed which improves the EE along with compensating for the degradation in SE, outage and SER performance.

- It has also been shown that the EE of the FD-MIMO-DF relay system depends on the total circuit power, which in turn depends on the number of active RF chains. Hence, employing S-ER further enhances the EE of the system through reducing the circuit power consumption by lowering the number of active RF chains.
- Closed-form expressions of SE, EE, outage probability and SER has been derived for the FD-MIMO-DF relay system for both fixed and the adaptive S-ER schemes.

C. ORGANIZATION AND NOTATIONS

The rest of this article is organized as follows: Section II provides an overview of the system model and the S-ER schemes. Closed-form expressions for SE, EE, outage and SER are derived in Section III. The simulation results are presented in Section IV, and finally, Section V concludes the paper.

The main notations of this paper are shown as: Matrices and vectors are represented by bold upper and lower cases respectively (e.g., $\mathbf{X}$ and $\mathbf{x}$). $\Gamma(\cdot)$ and $\Gamma(\cdot, \cdot)$ represents the gamma and the upper incomplete gamma function. $E[\cdot]$, $[\cdot]^H$, $tr[\cdot]$, $Pr[\cdot]$ represent the expectation operator, Hermitian, trace operator and probability respectively. $E_i(\cdot)$ is the exponential integral. Complex Gaussian distribution is represented with $\mathcal{CN}(\mu, \sigma^2)$, where μ is the mean and σ^2 denotes the variance.

II. SYSTEM MODEL

In this work, we consider a dual-hop communication between source and destination via relay, this can also be illustrated as Fig. 1. The source and destination are considered to be single-antenna and operating in a HD mode, whereas the relay is multi-antenna with N_t antennas at transmit-end and N_r antennas at receive-end, and is operating in a FD mode. Since the performance of the FD relay is impacted by the RSI, hence the received signal through the source-to-FD relay link experience interference from the SI. However, the relay-to-destination link is interference-free, i.e., the transmission of information from the FD relay node is not impacted by RSI. To exploit the above scenario, the proposed antenna allocation (AA) scheme allocates antennas at the FD relay node for information transmission/reception in an adaptive manner. Further, apart from information relaying, the FD relay also
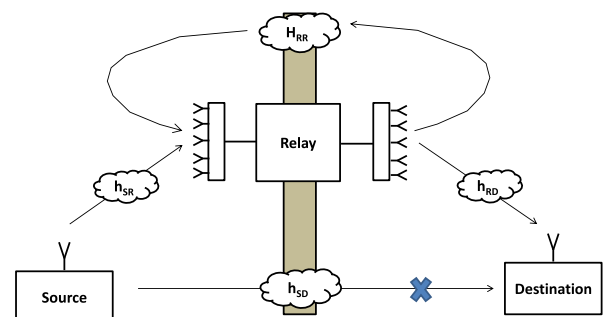

FIGURE 1. Schematic for the FD-MIMO-DF relay system model.

recycles a part of transmitted power through harvesting the SI by S-ER, which enhances the EE of the overall FD relay system.

A. ANTENNA ALLOCATION

The antennas at the FD relay can either be allotted for S-ER or information relaying at both transmit and receive end of the relay. The allocation of antennas at the FD relay is defined by an antenna allocation ratio, η_a, where $a \in (t, r)$ and t, r refers to the transmit and receiving ends of the FD relay respectively. This can be mathematically represented as: $\eta_a = N_a^{\text{S-ER}}/N_a$. Hence, the number of antennas for S-ER is $N_a^{S-ER} = \eta_a N_a$, and $N_a^I = (1 - \eta_a)N_a$ antennas are used for information relaying at both the transmit and receive-end of the FD relay. This has also been illustrated in Fig. 2.
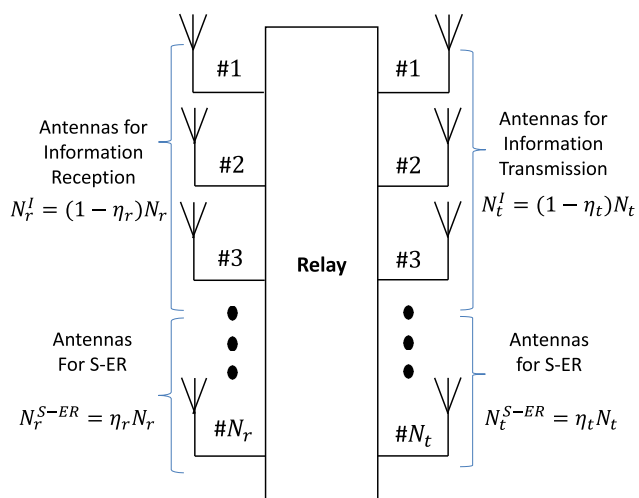

FIGURE 2. Illustration for the antenna allocation at the FD Relay for S-ER and information transmission and reception.

B. CHANNEL MODEL

The source-to-FD relay channel as well as FD relay-to-destination channel is modelled as flat Rayleigh fading channel denoted by $\mathbf{h}_{SR}$ and $\mathbf{h}_{RD}$ with dimensions $N_r^I \times 1$ and $1 \times N_t^I$ respectively. The channel elements of both $\mathbf{h}_{SR}$ and $\mathbf{h}_{RD}$ are independent and identically distributed (i.i.d.) with $\mathcal{CN}(0, 1)$. The transmit data symbol x_S is transmitted from the source, whereas the relay transmit $N_t^I \times 1$ transmit data vector which is denoted as $\mathbf{x}_R$, which may be thought as the time delayed and refined version of the data transmitted by the source. The elements of the transmit data are assumed to be i.i.d. with zero mean and variance $P_s = \mathrm{E}\left\{x_S x_S^H\right\}$ and $P_r = \mathrm{tr}\left(\mathrm{E}\left\{\mathbf{x}_R \mathbf{x}_R^H\right\}\right)$ respectively, where P_s and P_r are constrained by the total transmit power constraint at the source and the FD relay respectively. Furthermore, the $(\eta_t N_t + \eta_r N_r) \times N_t^I$ S-ER channel is modelled as flat Rayleigh fading channel denoted by $\mathbf{H}_{RR}$ with i.i.d. elements, $h_{i,j} \sim \mathcal{CN}(0, 1)$ [42]. Further, we assume that the direct link between the source and destination does not exist, or the direct path between the source and

destination is blocked due to obstacles, i.e., $h_{SD} = 0$. Hence, the transmission occurs through the relay only [22]. It is also assumed that full channel state information of source-to-FD relay channel ($\mathbf{h}_{SR}$), FD relay-to-destination channel ($\mathbf{h}_{RD}$) and the relay-to-relay channel ($\mathbf{H}_{RR}$) is available at the FD relay [28].

C. RESIDUAL SI MODEL

In FD systems, SI cancellation (SIC) is usually achieved in multiple stages. Passive SI suppression techniques like antenna separation, antenna isolation, etc., are capable of eliminating SI by 50 dB to 80 dB [43]. Further, analog and digital domain cancellations can mitigate up to $50 \sim 60$ dB SI [43].

In literature, residual self-interference (RSI) has been modeled in two ways.

- Fading Model: RSI is modelled by a statistical fading model like Rayleigh/Rician fading [21].
- Complex Gaussian Random Model: RSI is modelled as a Gaussian random variable with its variance depending on the underlying SIC methods.

Practical measurements have confirmed the Gaussian model [26], and it has been widely used in literature, thanks to its generality in modelling the RSI [20], [30], [31].[1] In the present work as well, RSI has been characterized by a complex Gaussian model.

D. S-ER SCHEMES

Two different ways are proposed to implement the S-ER scheme, namely adaptive and fixed S-ER scheme. This has also been illustrated in Fig. 3
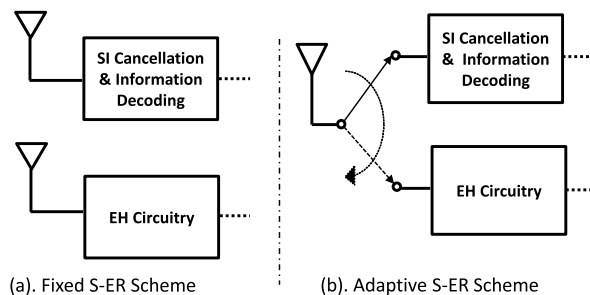

(a). Fixed S-ER Scheme   (b). Adaptive S-ER Scheme

FIGURE 3. Utilizing antenna for S-ER: (a) Fixed and (b) Adaptive S-ER scheme.

1) ADAPTIVE S-ER SCHEME

In the adaptive S-ER scheme, the N_t antennas at the transmit end of the FD relay are arranged in the decreasing order of channel gain. Then, the $N_t^I = (1 - \eta_t)N_t$ antennas corresponding to the largest channel gains are taken adaptively for

---

[1]The SI cancellation usually occurs in multiple stages, and there are imperfections associated with these schemes as well. As per the central limit theorem (CLT), the Gaussian assumption stands valid. Even if the assumptions are not correct, the Gaussian assumption can be considered as the lower bound of the performance [30].

information transmission while the remaining $N_t^{S-ER} = \eta_t N_t$ are utilized for S-ER.

2) FIXED S-ER SCHEME

In case of fixed S-ER scheme, the initial $N_t^I = (1 - \eta_t)N_t$ antennas out of N_t antennas are used for transmission purpose, while the remaining $N_t^{S-ER} = \eta_t N_t$ are utilized for S-ER scheme.

Similarly, the N_r antennas at the receive-end of the relay can be allocated for both the S-ER schemes.

E. RECEIVED SIGNAL MODEL

The $N_r^I \times 1$ received signal vector $\mathbf{y}_R$ at the relay can be expressed as

$$\mathbf{y}_R = \mathbf{h}_{SR}x_S + \mathbf{H}_{RR}\mathbf{x}_R + \mathbf{w}_R, \tag{1}$$

where $\mathbf{w}_R$ is the additive white Gaussian noise vector of dimension $N_r^I \times 1$ with its element being $\mathcal{CN}(0, \sigma^2)$. The received signal at the destination, y_D, can be expressed as

$$y_D = \mathbf{h}_{RD}\mathbf{x}_R + w_D, \tag{2}$$

where $w_D \sim \mathcal{CN}(0, \sigma^2)$ denotes the additive white Gaussian noise.

The self-interference component can be estimated at the FD relay since $\mathbf{x}_R$ is known to the relay. The estimated SI can be subtracted from the received signal. However, the complete cancellation of SI is inevitable due to the various imperfections associated with the estimation and cancellation. After subtracting the estimated SI from the received signal y_R in (1), the updated received signal can be rewritten as

$$\mathbf{y}_R = \mathbf{h}_{SR}x_S + \mathbf{d}_R + \mathbf{w}_R, \tag{3}$$

where $\mathbf{d}_R$ denotes the RSI vector of dimension $N_r^I \times 1$ with its element $d_R \sim \mathcal{CN}(0, \sigma_{rsi}^2)$ and $\sigma_{rsi}^2 = \alpha P_r^\nu$. The value of constants α and ν $(0 \leq \nu \leq 1)$ depends on the efficacy of the employed SI cancellation technique [30].

III. PERFORMANCE ANALYSIS

In this section, we derive the analytical expressions for the SE, outage, symbol error rate (SER) performance and EE for the adaptive S-ER as well as fixed S-ER schemes. Initially, the rate equations are formulated for both the source-to-FD relay and FD relay-to-destination links, which are utilized in deriving the SE as well as outage probability. Further, a circuit power consumption model is also discussed in detail. Based on the SE, S-ER and the power consumption model, the EE expressions are derived.

1) SPECTRAL EFFICIENCY

The normalized instantaneous rate R_{in} for the source-to-FD relay link can be formulated from (3), and can be expressed as

$$R_{SR}^{in} = \log_2 (1 + \rho_1(g)),$$

$$= \log_2 \left(1 + \frac{g_1 P_s}{\sigma_{rsi}^2 + \sigma^2}\right), \tag{4}$$

where $\rho_1(g)$ is the SINR at the FD relay, $g_1 = \sum_{i=1}^{N_r^I} |h_i|^2$ denotes the channel gain for the source-to-FD relay link based on maximal ratio combining and σ^2 denotes the additive noise variance. The average SE (ASE) of the source-to-FD relay link can be defined as

$$ASE_{SR} = \mathrm{E}\left[R_{SR}^{in}\right] = \mathrm{E}\left[\log_2 \left(1 + \frac{g_1 P_s}{\sigma_{rsi}^2 + \sigma^2}\right)\right]. \tag{5}$$

The closed-form expression for ASE of the source-to-FD relay link can be evaluated by solving the expectation over the distribution of channel gain g_1.

$$ASE_{SR} = \int_0^\infty \log_2 \left(1 + \frac{g_1 P_s}{\sigma_{rsi}^2 + \sigma^2}\right) f_G(g_1) dg_1. \tag{6}$$

Similarly, the normalized instantaneous rate R_{in} for the FD relay-to-destination link can be expressed as

$$R_{RD}^{in} = \log_2 (1 + \rho_2(g))$$

$$= \log_2 \left(1 + \frac{g_2 P_r}{\sigma^2}\right), \tag{7}$$

where $\rho_2(g)$ denotes the signal-to-noise ratio (SNR) at the destination, $g_2 = \sum_{i=1}^{N_I} |h_i|^2$, is the channel gain for the FD relay-to-destination link based on maximal ratio transmission. The ASE of the FD relay-to-destination link can be defined as

$$ASE_{RD} = \mathrm{E}\left[R_{RD}^{in}\right],$$

$$= \mathrm{E}\left[\log_2 \left(1 + \frac{g_2 P_r}{\sigma^2}\right)\right],$$

$$= \int_0^\infty \log_2 \left(1 + \frac{g_2 P_r}{\sigma^2}\right) f_G(g_2) dg_2. \tag{8}$$

Now based on DF protocol, the end-to-end (e2e) ASE of the source-to-destination link via FD relay can expressed as

$$ASE_{e2e} = \min \{ASE_{SR}, ASE_{RD}\}. \tag{9}$$

2) OUTAGE

The e2e outage from source-to-destination via FD relay P_{e2e} can be defined in the terms of P_{SR}^{out} and P_{RD}^{out} as

$$P_{e2e} = 1 - \left(1 - P_{SR}^{out}\right)\left(1 - P_{RD}^{out}\right),$$

$$= P_{SR}^{out} + P_{RD}^{out} - P_{SR}^{out} P_{RD}^{out}, \tag{10}$$

where P_{SR}^{out} is the outage probability for the source-to-FD relay link and P_{RD}^{out} is the outage probability for the FD relay-to-destination link.

The e2e outage can be evaluated in terms of a rate threshold, R_{th}, as discussed below. As a first step, we calculate the outage probability for the source-to-FD relay link, P_{SR}^{out}, which can be formulated as

$$P_{SR}^{out} = \Pr\left[R_{SR}^{in} < R_{th}\right]. \tag{11}$$

From (4), P_{SR}^{out} can be given as

$$P_{SR}^{out} = \Pr\left[\log_2\left(1 + \frac{g_1 P_s}{\sigma_{rsi}^2 + \sigma^2}\right) < R_{th}\right],$$

$$= \Pr\left[\frac{g_1 P_s}{\sigma_{rsi}^2 + \sigma^2} < 2^{R_{th}} - 1\right],$$

$$= \Pr\left[g_1 < \frac{(2^{R_{th}} - 1)(\sigma_{rsi}^2 + \sigma^2)}{P_s}\right],$$

$$= \Pr[g_1 < z_1], \quad (12)$$

where $z_1 = \frac{(2^{R_{th}}-1)(\sigma_{rsi}^2+\sigma^2)}{P_s}$.

Thus, the closed-form expression of the outage probability for the source-to-FD relay link can be evaluated as

$$P_{SR}^{out} = \int_0^{z_1} f_G(g_1) dg_1. \quad (13)$$

Similarly in the second step outage probability for the FD relay-to-destination link, P_{RD}^{out}, can be formulated as

$$P_{RD}^{out} = \Pr\left[R_{RD}^{in} < R_{th}\right]. \quad (14)$$

From (7), P_{RD}^{out} can be evaluated as

$$P_{RD}^{out} = \Pr\left[\log_2\left(1 + \frac{g_2 P_r}{\sigma^2}\right) < R_{th}\right],$$

$$= \Pr\left[\frac{g_2 P_r}{\sigma^2} < 2^{R_{th}} - 1\right],$$

$$= \Pr\left[g_2 < \frac{2^{R_{th}} - 1}{P_r/\sigma^2}\right],$$

$$= \Pr[g_2 < z_2], \quad (15)$$

where $z_2 = \frac{2^{R_{th}}-1}{P_r/N_o}$. Thus, the closed-form expression of the outage probability for the relay-to-destination link can be evaluated as

$$P_{RD}^{out} = \int_0^{z_2} f_G(g_2) dg_2. \quad (16)$$

3) SYMBOL ERROR RATE

In a dual-hop decode-and-forward communication the probability of symbol error is the complement of probability of correct reception. The probability of correct reception is the product of the probability of correct reception in the both the links of the dual-hop transmission [44]. So the e2e SER from source-to-destination via FD relay SER_{e2e} can be defined in the terms of SER^{SR} and SER^{RD} as

$$SER_{e2e} = 1 - (1 - SER_{SR})(1 - SER_{RD}),$$

$$= SER_{SR} + SER_{RD} - SER_{SR}SER_{RD}, \quad (17)$$

where SER_{SR} is the SER for the source-to-FD relay link and SER_{RD} is the SER for the relay-to-destination link.

Considering the M-QAM modulation scheme, the SER of the M-QAM data symbol from source-to-FD relay can be expressed as [45]

$$\Psi(\psi) = 1 - \left\{1 - \left(1 - \frac{1}{\sqrt{M}}\right) \text{erfc}\left(\sqrt{\frac{3\rho(\psi)}{2(M-1)}}\right)\right\}^2, \quad (18)$$

where erfc(.) is the complimentary error function [46, eq. (8.250.4)].

Therefore the average source-to-FD relay SER can be evaluated as

$$SER_{SR} = \text{E}[\Psi(g_1)],$$

$$= \int_0^\infty \Psi(g_1) f_G(g_1) dg_1. \quad (19)$$

Similarly the SER for the FD relay-to-destination link can be averaged across the fading channel and can be expressed as

$$SER_{RD} = \text{E}[\Psi(g_2)],$$

$$= \int_0^\infty \Psi(g_2) f_G(g_2) dg_2. \quad (20)$$

4) ENERGY EFFICIENCY

The average EE (AEE) can now be defined in bits/Joule/Hz as the ratio of ASE over the total power budget

$$AEE = \frac{ASE}{P_{tot} - P_{ser}}, \quad (21)$$

where P_{tot} is the total power consumed in transmission and circuitry at the source, FD relay and the destination, and P_{ser} is the harvested power through S-ER. The modelling of P_{tot} and P_{ser} are described as below.

a: POWER CONSUMPTION MODELLING

The power consumption at the source comprises of the transmission power, P_s, the power consumed by the high power amplifier (HPA) at the source P_{amp}^S, and the other circuit power P_c^S (excluding the HPA power consumption).[2] The power consumption of HPA is modelled as $P_{amp}^S = \beta P_s$, where $\beta = \frac{\varepsilon}{\varsigma} - 1$ and ε, ς are the peak-to-average ratio (PAR) and the drain efficiency of HPA, respectively. The value of β depends on modulation scheme and the associated constellation size.

Therefore, the source power consumption can be written as

$$P_{tot}^S = (1 + \beta)P_s + P_c^S, \quad (22)$$

which is a linear function over the transmission power at the source P_s. Since, the HPA is not present at the destination, the power consumption at the destination can be expressed as

$$P_{tot}^D = P_c^D, \quad (23)$$

where P_c^D is the circuit power consumption at the destination.

Since the relay is equipped with multiple-antennas, for the ease of exposition and without any loss of generality, it is assumed each of the active RF-chain consumes identical power [47]. So, the power consumption at the relay can be given as

$$P_{tot}^R = (1 + \beta)P_r + P_c^R, \quad (24)$$

where P_c^R is the circuit power consumption (excluding the HPA power consumption) at the FD relay.

---

[2]The other circuit power accounts for the power consumed by other blocks such as mixer, digital-to-analog converter, frequency synthesizer.

Further, since the relay needs extra power to cancel the RSI, denoting P_{SIC} as the SIC power required at the relay. Based on state-of-the-art SIC technologies discussed in literature, P_{SIC} can be modelled as a linear function over the P_r, so it can be expressed as below,

$$P_{SIC} = \alpha(1 + \beta)P_r + P_{c0}, \qquad (25)$$

where α is the isolating factor, and P_{c0} comprises of all other constant power consumption in the analog and digital SI cancellation circuit [48].

Thus, the total circuit power consumption of FD relay system can be expressed as

$$P_c^{FD} = P_c^S + P_c^R + P_c^D + P_{SIC}. \qquad (26)$$

Further, expressing $P_t = P_s + P_r$ as the total transmit power, the total power consumption in the FD relay system, P_{tot}, can be written as:

$$P_{tot} = (1 + \beta)P_t + P_c^{FD}. \qquad (27)$$

b: SELF-ENERGY RECYCLING
The FD relay node not only collects the transmitted signal from the source node, but also recycles part of its transmitted power as few of the antennas are being activated at the same time for the energy harvesting purpose. In the remaining antennas FD relay employs self-interference cancellation (SIC) techniques to eliminate the SI signal [32]. The harvested energy at relay will be stored in the battery, which prolongs the battery life at the FD-relay [49]. So, in the S-ER process, ηN_t antennas are allotted for S-ER out of N_t antennas at the FD relay transmit-end. The amount of power harvested through S-ER can be expressed as

$$
\begin{aligned}
P_{ser} &= \kappa \times \mathrm{E}\left[\mathrm{tr}\left\{ \mathbf{H}_{RR}\mathbf{Q}_{xx}(\mathbf{H}_{RR})^H \right\} \right], \\
&= \kappa(\eta_t N_t + \eta_r N_r)(1 - \eta_t)N_t P_r, \qquad (28)
\end{aligned}
$$

where $\mathbf{Q}_{xx} = \mathrm{E}\left\{ \mathbf{x}_R \mathbf{x}_R^H \right\}$ is the co-variance matrix for relay transmitted signal $\mathbf{x}_R$ and κ is the RF-to-DC conversion efficiency [50]. Since the strength of received SI is several order larger than the strength of the received signal from source, its contribution can be neglected in the harvested energy.

Now, based on the above formulations of SE, outage, SER and the EE, the subsequent subsections present the detailed derivation of the closed-form expressions of these quantities. Subsection-A comprises the derivations corresponding to the adaptive S-ER scheme, whereas the fixed S-ER scheme is discussed in Subsection-B.

A. ADAPTIVE S-ER SCHEME
In the adaptive S-ER scheme, the antennas for information transmission at the FD relay are allocated adaptively based on the channel gain. So, the distribution of the channel gain for transmit antenna selection can be invoked utilizing the results derived in ordered statistics. From [51], the effective probability density function (PDF) for the sum of L_s largest

exponentially distributed random variable out of L random variables can be given as

$$
\begin{aligned}
&f_{\Sigma}(\gamma) \\
&= \binom{L}{L_s}\left[\frac{e^{-\gamma}\gamma^{L_s-1}}{(L_s-1)!} + \sum_{\tau=1}^{L-L_s}(-1)^{L_s+\tau-1}\binom{L-L_s}{\tau} \right. \\
&\quad \left. \times \left(\frac{L_s}{\tau}\right)^{L_s-1} e^{-\gamma}\left\{ e^{\frac{-(\tau\gamma)}{L_s}} - \sum_{m=0}^{L_s-2}\frac{1}{m!}\left(\frac{-\tau\gamma}{L_s}\right)^m \right\} \right].
\end{aligned}
\qquad (29)
$$

The above PDF, as described in (29), is utilized to evaluate the performance of adaptive S-ER scheme in terms of SE, outage, SER and the EE.

1) SPECTRAL EFFICIENCY FOR ADAPTIVE S-ER SCHEME
From (6), the closed-form expression for ASE of the source-to-FD relay link can be evaluated as

$$ASE_{SR} = \int_0^\infty \log_2\left(1 + \frac{g_1 P_s}{\sigma_{rsi}^2 + \sigma^2}\right) f_G(g_1)dg_1, \qquad (30)$$

or equivalently

$$ASE_{SR} = \frac{1}{\ln 2}\int_0^\infty \ln(1 + g_1 A_1) f_G(g_1)dg_1, \qquad (31)$$

where $A_1 = \frac{P_s}{\sigma_{rsi}^2 + \sigma^2}$.

Now by substituting (29), the above expression can be expanded as

$$
\begin{aligned}
ASE_{SR} &= \frac{1}{\ln 2}\int_0^\infty \ln(1 + g_1 A_1) \binom{N_r}{N_r^I}e^{-g_1} \\
&\times \left[\frac{g_1^{N_r^I-1}}{(N_r^I-1)!} + \sum_{\tau=1}^{\eta N_r}(-1)^{N_r^I+\tau-1}\left(\frac{N_r^I}{\tau}\right)^{N_r^I-1} \right. \\
&\times \left. \binom{\eta N_r}{\tau}\left\{ e^{\frac{-(\tau g_1)}{N_r^I}} - \sum_{m=0}^{N_r^I-2}\frac{1}{m!}\left(\frac{-\tau g_1}{N_r^I}\right)^m \right\} \right] dg_1.
\end{aligned}
\qquad (32)
$$

After some mathematical manipulations, (32) can be reformulated as

$$
\begin{aligned}
ASE_{SR} &= \frac{1}{\ln 2}\binom{N_r}{N_r^I}\left[\int_0^\infty \frac{e^{-g_1}\ln(1 + g_1 A_1)g_1^{N_r^I-1}}{(N_r^I-1)!}dg_1 \right. \\
&+ \sum_{\tau=1}^{\eta N_r}\Xi_1(\tau)\left\{ \int_0^\infty \ln(1 + g_1 A_1)e^{-g_1}e^{\frac{-(\tau g_1)}{N_r^I}}dg_1 \right. \\
&- \left. \left. \sum_{m=0}^{N_r^I-2}\Xi_2(m)\int_0^\infty \ln(1 + g_1 A_1)e^{-g_1}g_1^m dg_1 \right\} \right],
\end{aligned}
\qquad (33)
$$

where

$$\Xi_1(\tau) = (-1)^{N_r^I+\tau-1}\left(\frac{N_r^I}{\tau}\right)^{N_r^I-1}\binom{\eta N_r}{\tau} \qquad (34)$$

and

$$\Xi_2(m) = \frac{1}{m!}\left(\frac{-\tau}{N_r^I}\right)^m, \qquad (35)$$

or equivalently

$$ASE_{SR} = \frac{1}{\ln 2}\binom{N_r}{N_r^I}\left[\frac{1}{(N_r^I-1)!}\mathcal{I}_1\right.$$
$$\left.+ \sum_{\tau=1}^{\eta N_r}\Xi_1(\tau)\left\{\mathcal{I}_2 - \sum_{m=0}^{N_r^I-2}\Xi_2(m)\mathcal{I}_3\right\}\right], \qquad (36)$$

with

$$\mathcal{I}_1 = \int_0^\infty e^{-g_1}\ln(1+g_1 A_1)g_1^{N_r^I-1}dg_1, \qquad (37)$$

$$\mathcal{I}_2 = \int_0^\infty \ln(1+g_1 A_1)e^{\frac{-(\tau+N_r^I)}{N_r^I}g_1}dg_1 \qquad (38)$$

and

$$\mathcal{I}_3 = \int_0^\infty \ln(1+g_1 A_1)e^{-g_1}g_1^m dg_1. \qquad (39)$$

Using [52, Appendix A] and [46, eq. (4.337.2)], $\mathcal{I}_1$, $\mathcal{I}_2$ and $\mathcal{I}_3$ can be evaluated as

$$\mathcal{I}_1 = (N_r-1)!\exp\left(\frac{1}{A_1}\right)\sum_{k=0}^{N_r^I-1}\mathrm{E}_{k+1}\left(\frac{1}{A_1}\right), \qquad (40)$$

$$\mathcal{I}_2 = -\frac{N_r^I}{\tau+N_r^I}\exp\left(\frac{\tau+N_r^I}{N_r^I A_1}\right)\mathrm{E}_i\left(\frac{-(\tau+N_r^I)}{N_r^I A_1}\right) \qquad (41)$$

and

$$\mathcal{I}_3 = (m)!\exp\left(\frac{1}{A_1}\right)\sum_{k=0}^{m}\mathrm{E}_{k+1}\left(\frac{1}{A_1}\right), \qquad (42)$$

where the exponential integral $\mathrm{E}_\varpi(\theta)$ denotes a special case of complementary incomplete gamma function defined as [52]

$$\mathrm{E}_\varpi(\theta) = \theta^{(\varpi-1)}\Gamma(1-\varpi,\theta), \qquad (43)$$

for $\varpi = 0,1,2\ldots$ and $Re(\theta) > 0$.

Finally by substituting $\mathcal{I}_1$, $\mathcal{I}_2$, $\mathcal{I}_3$, Ξ_1 and Ξ_2 in (36) and rearranging the terms, the closed-form expression for ASE of the source-to-FD relay link can be expressed as

$$ASE_{SR} = \frac{1}{\ln 2}\binom{N_r}{N_r^I}\left[\exp\left(\frac{1}{A_1}\right)\sum_{k=0}^{N_r^I-1}\mathrm{E}_{k+1}\left(\frac{1}{A_1}\right)\right.$$
$$+ \sum_{\tau=1}^{N_r-N_r^I}(-1)^{N_r^I+\tau-1}\binom{N_r-N_r^I}{\tau}\left(\frac{N_r^I}{\tau}\right)^{N_r^I-1}$$
$$\times\left\{\frac{-N_r^I}{\tau+N_r^I}\exp\left(\frac{\tau+N_r^I}{N_r^I A_1}\right)\mathrm{E}_i\left(\frac{-(\tau+N_r^I)}{N_r^I A_1}\right)\right.$$
$$\left.\left.- \sum_{m=0}^{N_r^I-2}\left(\frac{-\tau}{N_r^I}\right)^m\exp\left(\frac{1}{A_1}\right)\sum_{k=0}^{m}\mathrm{E}_{k+1}\left(\frac{1}{A_1}\right)\right\}\right]. \qquad (44)$$

Now the closed-form expression for ASE of the FD relay-to-destination link as defined in (8) can be formulated identically by utilizing (29) as

$$ASE_{RD} = \int_0^\infty \log_2\left(1+\frac{g_2 P_r}{\sigma^2}\right)f_G(g_2)dg_2, \qquad (45)$$

or equivalently

$$ASE_{RD} = \frac{1}{\ln 2}\int_0^\infty \ln(1+g_2 A_2)f_G(g_2)dg_2, \qquad (46)$$

where $A_2 = \frac{P_r}{\sigma^2}$. Now by substituting (29), the above expression can be expanded as

$$ASE_{RD} = \frac{1}{\ln 2}\int_0^\infty \ln(1+g_2 A_2)\binom{N_t}{N_t^I}e^{-g_2}\left[\frac{g_2^{N_t^I-1}}{(N_t^I-1)!}\right.$$
$$+ \sum_{\tau=1}^{\eta N_t}(-1)^{N_t^I+\tau-1}\binom{\eta N_t}{\tau}\left(\frac{N_t^I}{\tau}\right)^{N_t^I-1}$$
$$\left.\times\left\{e^{\frac{-(\tau g_2)}{N_t^I}} - \sum_{m=0}^{N_t^I-2}\frac{1}{m!}\left(\frac{-\tau g_2}{N_t^I}\right)^m\right\}\right]dg_2, \qquad (47)$$

which can be solved based on a similar approach that has been undertaken above while evaluating the expression in (32). Thus, the closed-form expression for the ASE of the FD relay-to-destination link, ASE_{RD}, can be expressed as

$$ASE_{RD} = \frac{1}{\ln 2}\binom{N_t}{N_t^I}\left[\exp\left(\frac{1}{A_2}\right)\sum_{k=0}^{N_t^I-1}\mathrm{E}_{k+1}\left(\frac{1}{A_2}\right)\right.$$
$$+ \sum_{\tau=1}^{N_t-N_t^I}(-1)^{N_t^I+\tau-1}\binom{N_t-N_t^I}{\tau}\left(\frac{N_t^I}{\tau}\right)^{N_t^I-1}$$
$$\times\left\{\frac{-N_t^I}{\tau+N_t^I}\exp\left(\frac{\tau+N_t^I}{N_t^I A_2}\right)\mathrm{E}_i\left(\frac{-(\tau+N_t^I)}{N_t^I A_2}\right)\right.$$
$$\left.\left.- \sum_{m=0}^{N_t^I-2}\left(\frac{-\tau}{N_t^I}\right)^m\exp\left(\frac{1}{A_2}\right)\sum_{k=0}^{m}\mathrm{E}_{k+1}\left(\frac{1}{A_2}\right)\right\}\right], \qquad (48)$$

where $A_2 = \frac{P_r}{\sigma^2}$.

So, the e2e ASE of the source-to-destination link for adaptive S-ER scheme, ASE_{e2e}^{adp} can now be expressed as

$$ASE_{e2e}^{adp} = \min\{ASE_{SR}, ASE_{RD}\}. \qquad (49)$$

2) ENERGY EFFICIENCY FOR ADAPTIVE S-ER SCHEME

The AEE for adaptive S-ER scheme, AEE_{e2e}^{adp}, as defined in (21) can now be evaluated by utilizing (27), (28), and (49). Hence, it can be written as

$$AEE_{e2e}^{adp} = \frac{ASE_{e2e}^{adp}}{(1+\beta)P_t + P_c^{FD} - \kappa(\eta_t N_t + \eta_r N_r)(1-\eta_t)N_t P_R}. \qquad (50)$$

3) OUTAGE FOR ADAPTIVE S-ER SCHEME

The outage probability for the source-to-FD relay link P_{SR}^{out} as defined in (13) can be evaluated as

$$P_{SR}^{out} = \int_0^{z_1} f_G(g_1) dg_1, \tag{51}$$

which by utilizing (29) can be re-written as

$$
P_{SR}^{out} = \int_0^{z_1} \binom{N_r}{N_r^I} \left[\frac{g_1^{N_r^I-1}}{(N_r^I-1)!} e^{-g_1} + \sum_{\tau=1}^{\eta N_r} (-1)^{N_r^I+\tau-1} \right.
$$
$$
\times \binom{\eta N_r}{\tau} \left(\frac{N_r^I}{\tau} \right)^{N_r^I-1} e^{-g_1} \left\{ e^{\frac{-(\tau g_1)}{N_r^I}} \right.
$$
$$
\left. \left. - \sum_{m=0}^{N_r^I-2} \frac{1}{m!} \left(\frac{-\tau g_1}{N_r^I} \right)^m \right\} \right] dg_1. \tag{52}
$$

After some mathematical manipulations (52) can be reformulated as

$$
P_{SR}^{out} = \binom{N_r}{N_r^I} \left[\frac{1}{(N_r^I-1)!} \int_0^{z_1} g_1^{N_r^I-1} e^{-g_1} dg_1 \right.
$$
$$
+ \sum_{\tau=1}^{\eta N_r} \Xi_1(\tau) \left\{ \int_0^{z_1} e^{\frac{-(\tau g_1)}{N_r^I}} e^{-g_1} dg_1 \right.
$$
$$
\left. \left. - \sum_{m=0}^{N_r^I-2} \Xi_2 \int_0^{z_1} (m) g_1^m e^{-g_1} dg_1 \right\} \right], \tag{53}
$$

where

$$\Xi_1(\tau) = (-1)^{N_r^I+\tau-1} \left(\frac{N_r^I}{\tau} \right)^{N_r^I-1} \binom{\eta N_r}{\tau} \tag{54}$$

and

$$\Xi_2(m) = \frac{1}{m!} \left(\frac{-\tau}{N_r^I} \right)^m, \tag{55}$$

or equivalently

$$
P_{SR}^{out} = \binom{N_r}{N_r^I} \left[\frac{1}{(N_r^I-1)!} \mathcal{J}_1 \right.
$$
$$
\left. + \sum_{\tau=1}^{\eta N_r} \Xi_1(\tau) \left\{ \mathcal{J}_2 - \sum_{m=0}^{N_r^I-2} \Xi_2(m) \mathcal{J}_3 \right\} \right], \tag{56}
$$

with

$$\mathcal{J}_1 = \int_0^{z_1} g_1^{N_r^I-1} e^{-g_1} dg_1, \tag{57}$$

$$\mathcal{J}_2 = \int_0^{z_1} e^{\frac{-(\tau+1)g_1}{N_r^I}} dg_1, \tag{58}$$

and

$$\mathcal{J}_3 = \int_0^{z_1} g_1^m e^{-g_1} dg_1. \tag{59}$$

Now by using [46, eq. (3.351.1)], $\mathcal{J}_1$, $\mathcal{J}_2$ and $\mathcal{J}_3$ can be evaluated as:

$$\mathcal{J}_1 = (N_r^I-1)! - \exp(-z_1) \sum_{\omega=0}^{N_r^I-1} \frac{(N_r^I-1)!}{\omega!} z_1^\omega, \tag{60}$$

$$\mathcal{J}_2 = \frac{1 - \exp\left\{-z_1\left(1 + \frac{\tau}{N_r^I}\right)\right\}}{\left(1 + \frac{\tau}{N_r^I}\right)} \tag{61}$$

and

$$\mathcal{J}_3 = (m)! - \exp(-z_1) \sum_{\omega=0}^{m} \frac{(m)!}{\omega!} z_1^\omega. \tag{62}$$

Finally by substituting $\mathcal{J}_1$, $\mathcal{J}_2$, $\mathcal{J}_3$, Ξ_1 and Ξ_2 in (56) and rearranging the terms, the closed form expression for the outage probability for the source-to-FD relay, P_{SR}^{out} can now be expressed as

$$
P_{SR}^{out} = \binom{N_r}{N_r^I} \left[1 - \exp(-z_1) \sum_{\omega=0}^{N_r^I-1} \frac{z_1^\omega}{\omega!} + \sum_{\tau=1}^{\eta N_r} (-1)^{N_r^I+\tau-1} \right.
$$
$$
\times \binom{\eta N_r}{\tau} \left(\frac{N_r^I}{\tau} \right)^{N_r^I-1} \left\{ \frac{1 - \exp\left\{-z_1\left(1 + \frac{\tau}{N_r^I}\right)\right\}}{\left(1 + \frac{\tau}{N_r^I}\right)} \right.
$$
$$
\left. \left. - \sum_{m=0}^{N_r^I-2} \left(\frac{-\tau}{N_r^I} \right)^m \left(1 - \exp(-z_1) \sum_{\omega=0}^{m} \frac{z_1^\omega}{\omega!} \right) \right\} \right]. \tag{63}
$$

Similarly, the outage probability for the FD relay-to-destination link P_{RD}^{out} as defined in (16) can be formulated as

$$P_{RD}^{out} = \int_0^{z_2} f_G(g_2) dg_2, \tag{64}$$

which by utilizing (29) can be re-written as

$$
P_{RD}^{out} = \int_0^{z_2} \binom{N_t}{N_t^I} \left[\frac{e^{-g_2} g_2^{N_t^I-1}}{(N_t^I-1)!} + \sum_{\tau=1}^{\eta N_t} (-1)^{N_t^I+\tau-1} \right.
$$
$$
\times \binom{\eta N_t}{\tau} \left(\frac{N_t^I}{\tau} \right)^{N_t^I-1} e^{-g_2} \left\{ e^{\frac{-(\tau g_2)}{N_t^I}} \right.
$$
$$
\left. \left. - \sum_{m=0}^{N_t^I-2} \frac{1}{m!} \left(\frac{-\tau g_2}{N_t^I} \right)^m \right\} \right] dg_2. \tag{65}
$$

Similar to (52), the integral in (65) can be evaluated; thus, the closed form expression for the outage probability for the FD relay-to-destination link, P_{RD}^{out}, can be expressed as

$$
P_{RD}^{out} = \binom{N_t}{N_t^I} \left[1 - \exp(-z_2) \sum_{\omega=0}^{N_t^I-1} \frac{z_2^\omega}{\omega!} \right.
$$
$$
+ \sum_{\tau=1}^{\eta N_t} (-1)^{N_t^I+\tau-1} \binom{\eta N_t}{\tau} \left(\frac{N_t^I}{\tau} \right)^{N_t^I-1}
$$
$$
\times \left\{ \frac{1 - \exp\left\{-z_2\left(1 + \frac{\tau}{N_t^I}\right)\right\}}{\left(1 + \frac{\tau}{N_t^I}\right)} \right.
$$
$$
\left. \left. - \sum_{m=0}^{N_t^I-2} \left(\frac{-\tau}{N_t^I} \right)^m \left(1 - \exp(-z_2) \sum_{\omega=0}^{m} \frac{z_2^\omega}{\omega!} \right) \right\} \right]. \tag{66}
$$

So the e2e outage probability, i.e., of the source-to-destination link via relay, for adaptive S-ER scheme P_{e2e}^{adp} can be evaluated by substituting (63) and (66) in (10). Hence, this can be expressed as

$$P_{e2e}^{adp} = P_{SR}^{out} + P_{RD}^{out} - P_{SR}^{out} P_{RD}^{out}. \tag{67}$$

4) SYMBOL ERROR RATE FOR ADAPTIVE S-ER SCHEME

Utilizing (18), the SER for the source-to-FD relay link as defined in (19) can be evaluated as

$$SER_{SR} = \int_0^\infty \left[1 - \left\{ 1 - \left(1 - \frac{1}{\sqrt{M}} \right) \right. \right.$$
$$\left. \left. \times \; \mathrm{erfc} \left(\sqrt{\frac{3\rho(g_1)}{2(M-1)}} \right) \right\}^2 \right] f_G(g_1) dg_1. \tag{68}$$

The analytical expression of SER in (68) is intractable. However, it can be evaluated by approximating (18) as [53, eq. (33)]

$$\Psi(\psi) \approx 2 \left(1 - \frac{1}{\sqrt{M}} \right) \mathrm{erfc} \left(\sqrt{\frac{3\rho(\psi)}{2(M-1)}} \right). \tag{69}$$

Using (69), the SER can be averaged across the fading channel and can be rewritten as

$$SER_{SR} \approx \int_0^\infty \Upsilon \mathrm{erfc} \left(\sqrt{\frac{3\rho(g_1)}{2(M-1)}} \right) f_G(g_1) dg_1$$
$$\approx \int_0^\infty \Upsilon \left\{ 1 - \mathrm{erf} \left(\sqrt{\frac{3\rho(g_1)}{2(M-1)}} \right) \right\} f_G(g_1) dg_1$$
$$\approx \Upsilon \left[1 - \int_0^\infty \mathrm{erf} \left(\sqrt{\frac{3\rho(g_1)}{2(M-1)}} \right) f_G(g_1) dg_1 \right] \tag{70}$$

where $\Upsilon = 2 \left(1 - \frac{1}{\sqrt{M}} \right)$, $\mathrm{erf}(.) = (1 - \mathrm{erfc}(.))$ is the error function [46, eq. (8.250.1)].

The SER for the source-to-FD relay link SER_{SR} in (70) can now be evaluated by utilizing (29) as

$$SER_{SR}$$
$$= \Upsilon \left[1 - \binom{N_r}{N_r^I} \int_0^\infty \mathrm{erf} \left(\sqrt{g_1 \Omega_1} \right) e^{-g_1} \right.$$
$$\times \left\{ \frac{g_1^{N_r^I-1}}{(N_r^I-1)!} + \sum_{\tau=1}^{\eta N_r} (-1)^{N_r^I+\tau-1} \binom{\eta N_r}{\tau} \left(\frac{N_r^I}{\tau} \right)^{N_r^I-1} \right.$$
$$\left. \left. \times \left(e^{\frac{-(\tau g_1)}{N_r^I}} - \sum_{m=0}^{N_r^I-2} \frac{1}{m!} \left(\frac{-\tau g_1}{N_r^I} \right)^m \right) \right\} dg_1 \right], \tag{71}$$

where

$$\Omega_1 = \frac{3P_s}{2 \left(\sigma_{rsi}^2 + \sigma^2 \right) (M-1)}. \tag{72}$$

Substituting $\Omega_1 = \Lambda_1^2$, $g_1 = \varphi_1^2$ in (71), it can be reformulated as

$$SER_{SR}$$
$$= \Upsilon \left[1 - 2 \binom{N_r}{N_r^I} \int_0^\infty \mathrm{erf} \left(\Lambda_1 \varphi_1 \right) \left\{ \frac{\varphi_1^{2N_r^I-1} e^{-\varphi_1^2}}{(N_r^I-1)!} \right. \right.$$
$$+ \sum_{\tau=1}^{\eta N_r} (-1)^{N_r^I+\tau-1} \binom{\eta N_r}{\tau} \left(\frac{N_r^I}{\tau} \right)^{N_r^I-1} \left(\varphi_1 e^{-\varphi_1^2 \frac{(\tau+N_r^I)}{N_r^I}} \right.$$
$$\left. \left. \left. - \sum_{m=0}^{N_r^I-2} \frac{1}{m!} \left(\frac{-\tau}{N_r^I} \right)^m \varphi_1^{2m+1} e^{-\varphi_1^2} \right) \right\} d\varphi_1 \right], \tag{73}$$

or equivalently

$$SER_{SR} = \Upsilon \left\{ 1 - 2 \binom{N_r}{N_r^I} \mathcal{K} \right\}, \tag{74}$$

where

$$\mathcal{K}$$
$$= \int_0^\infty \mathrm{erf} \left(\Lambda_1 \varphi_1 \right) \left\{ \frac{\varphi_1^{2N_r^I-1} e^{-\varphi_1^2}}{(N_r^I-1)!} + \sum_{\tau=1}^{\eta N_r} \Xi_1 (\tau) \right.$$
$$\left. \times \left(\varphi_1 e^{-\varphi_1^2 \frac{(\tau+N_r^I)}{N_r^I}} - \sum_{m=0}^{N_r^I-2} \Xi_2 (m) \varphi_1^{2m+1} e^{-\varphi_1^2} \right) \right\} d\varphi_1, \tag{75}$$

with

$$\Xi_1 (\tau) = (-1)^{N_r^I+\tau-1} \left(\frac{N_r^I}{\tau} \right)^{N_r^I-1} \binom{\eta N_r}{\tau} \tag{76}$$

and

$$\Xi_2 (m) = \frac{1}{m!} \left(\frac{-\tau}{N_r^I} \right)^m. \tag{77}$$

Now by some mathematical manipulations (74) can be re-written as

$$\mathcal{I} = \frac{1}{(N_r^I-1)!} \int_0^\infty \mathrm{erf} \left(\Lambda_1 \varphi_1 \right) \varphi_1^{2N_r^I-1} e^{-\varphi_1^2} d\varphi_1$$
$$+ \sum_{\tau=1}^{\eta N_r} \Xi_1 (\tau) \left\{ \int_0^\infty \mathrm{erf} \left(\Lambda_1 \varphi_1 \right) \varphi_1 e^{-\varphi_1^2 \frac{(\tau+N_r^I)}{N_r^I}} d\varphi_1 \right.$$
$$\left. - \sum_{m=0}^{N_r^I-2} \Xi_2 (m) \int_0^\infty \mathrm{erf} \left(\Lambda_1 \varphi_1 \right) \varphi_1^{2m+1} e^{-\varphi_1^2} d\varphi_1 \right\}, \tag{78}$$

or equivalently

$$\mathcal{I} = \frac{1}{(N_r^I-1)!} \mathcal{I}_1 + \sum_{\tau=1}^{\eta N_r} \Xi_1 (\tau) \left\{ \mathcal{I}_2 - \sum_{m=0}^{N_r^I-2} \Xi_2 (m) \mathcal{I}_3 \right\}, \tag{79}$$

where

$$\mathcal{I}_1 = \int_0^\infty \varphi_1^{2N_r^I-1} e^{-\varphi_1^2} \mathrm{erf} \left(\Lambda_1 \varphi_1 \right) d\varphi_1 \tag{80}$$

$$\mathcal{I}_2 = \int_0^\infty \varphi_1 e^{-\varphi_1^2 \frac{(\tau + N_r^I)}{N_r^I}} \operatorname{erf}(\Lambda_1 \varphi_1) \, d\varphi_1 \tag{81}$$

and

$$\mathcal{I}_3 = \int_0^\infty \varphi_1^{2m+1} e^{-\varphi_1^2} \operatorname{erf}(\Lambda_1 \varphi_1) \, d\varphi_1 \tag{82}$$

Utilizing [54, eq. (4.3.4), (4.3.8)], $\mathcal{I}_1$, $\mathcal{I}_2$ and $\mathcal{I}_3$ can be solved as

$$\mathcal{I}_1 = \frac{\Lambda_1}{\sqrt{\pi}} \Gamma\left(N_r^I + \frac{1}{2}\right) {}_2F_1\left(\frac{1}{2}, N_r^I + \frac{1}{2}; \frac{3}{2}; -\Omega_1\right) \tag{83}$$

,

$$\mathcal{I}_2 = \frac{\Lambda_1}{2} \frac{N_r^I}{N_r^I + \tau} \frac{1}{\sqrt{\Lambda_1^2 + \frac{N_r^I + \tau}{N_r^I}}} \tag{84}$$

and

$$\mathcal{I}_3 = \frac{\Lambda_1}{\sqrt{\pi}} \Gamma\left(m + \frac{3}{2}\right) {}_2F_1\left(\frac{1}{2}, m + \frac{3}{2}; \frac{3}{2}; -\Omega_1\right). \tag{85}$$

After substituting the values of $\mathcal{I}_1$, $\mathcal{I}_2$, $\mathcal{I}_3$, Ξ_1 and Ξ_2 in (79) and rearranging the terms, the closed form expression for the SER of the source-to-FD relay link can be expressed as

$$SER_{SR} = \Upsilon \left[1 - 2\binom{N_r}{N_r^I} \sqrt{\frac{\Omega_1}{\pi}} \left\{ \frac{\Gamma\left(N_r^I + \frac{1}{2}\right)}{(N_r^I - 1)!} \Theta_1 \right. \right.$$
$$+ \sum_{\tau=1}^{\eta N_r} (-1)^{N_r^I + \tau - 1} \binom{\eta N_r}{\tau} \left(\frac{N_r^I}{\tau}\right)^{N_r^I - 1}$$
$$\times \left(\sqrt{\frac{\pi}{4}} \frac{N_r^I}{N_r^I + \tau} \frac{1}{\sqrt{\Omega_1 + \frac{N_r^I + \tau}{N_r^I}}} \right.$$
$$\left. \left. \left. - \sum_{m=0}^{N_r^I - 2} \frac{1}{m!} \left(\frac{-\tau}{N_r^I}\right)^m \Gamma\left(m + \frac{3}{2}\right) \Theta_2 \right) \right\} \right], \tag{86}$$

with

$$\Theta_1 = {}_2F_1\left(\frac{1}{2}, N_r^I + \frac{1}{2}; \frac{3}{2}; -\Omega_1\right) \tag{87}$$

and

$$\Theta_2 = {}_2F_1\left(\frac{1}{2}, m + \frac{3}{2}; \frac{3}{2}; -\Omega_1\right), \tag{88}$$

where $_2F_1(.)$ denotes the hyper-geometric function as defined in [46, 9.14.1].

Similarly the SER for the FD relay-to-destination link SER_{RD} as defined in (20) can be formulated in the similar fashion and can be evaluated by utilizing (29) and (70) as

$$SER_{RD}$$
$$= \Upsilon \left[1 - \binom{N_t}{N_t^I} \int_0^\infty \operatorname{erf}\left(\sqrt{g_2 \Omega_2}\right) e^{-g_2} \right.$$
$$\times \left\{ \frac{g_2^{N_t^I - 1}}{(N_t^I - 1)!} + \sum_{\tau=1}^{\eta N_t} (-1)^{N_t^I + \tau - 1} \binom{\eta N_t}{\tau} \left(\frac{N_t^I}{\tau}\right)^{N_t^I - 1} \right.$$

$$\times \left(e^{\frac{-(\tau g_2)}{N_t^I}} - \sum_{m=0}^{N_t^I - 2} \frac{1}{m!} \left(\frac{-\tau g_2}{N_t^I}\right)^m \right) \right\} dg_2 \right], \tag{89}$$

where $\Omega_2 = \frac{3P_r}{2(\sigma^2)(M-1)}$.

On substituting $\Omega_2 = \Lambda_2^2$, $g_2 = \varphi_2^2$ in (89), it can be reformulated as

$$SER_{RD} = \Upsilon \left[1 - 2\binom{N_t}{N_t^I} \int_0^\infty \operatorname{erf}(\Lambda_2 \varphi_2) \right.$$
$$\times \left\{ \frac{e^{-\varphi_2^2} \varphi_2^{2N_t^I - 1}}{(N_t^I - 1)!} + \sum_{\tau=1}^{\eta N_t} (-1)^{N_t^I + \tau - 1} \binom{\eta N_t}{\tau} \right.$$
$$\times \left(\frac{N_t^I}{\tau}\right)^{N_t^I - 1} \left(\varphi_2 e^{-\varphi_2^2 \frac{(\tau + N_t^I)}{N_t^I}} \right.$$
$$\left. \left. - \sum_{m=0}^{N_t^I - 2} \frac{1}{m!} \left(\frac{-\tau}{N_t^I}\right)^m \varphi_2^{2m+1} e^{-\varphi_2^2} \right) \right\} d\varphi_2 \right]. \tag{90}$$

Equation (90) is identical to (73) and can be solved through a similar approach, thus the closed-form expression for the SER of FD relay-to-destination can be expressed as

$$SER_{RD} = \Upsilon \left[1 - 2\binom{N_t}{N_t^I} \sqrt{\frac{\Omega_2}{\pi}} \left\{ \frac{\Gamma\left(N_t^I + \frac{1}{2}\right)}{(N_t^I - 1)!} \Theta_3 \right. \right.$$
$$+ \sum_{\tau=1}^{\eta N_t} (-1)^{N_t^I + \tau - 1} \binom{\eta N_t}{\tau} \left(\frac{N_t^I}{\tau}\right)^{N_t^I - 1}$$
$$\times \left(\sqrt{\frac{\pi}{4}} \frac{N_t^I}{N_t^I + \tau} \frac{1}{\sqrt{\Omega_2 + \frac{N_t^I + \tau}{N_t^I}}} \right.$$
$$\left. \left. \left. - \sum_{m=0}^{N_t^I - 2} \frac{1}{m!} \left(\frac{-\tau}{N_t^I}\right)^m \Gamma\left(m + \frac{3}{2}\right) \Theta_4 \right) \right\} \right], \tag{91}$$

where $\Theta_3 = {}_2F_1\left(\frac{1}{2}, N_t^I + \frac{1}{2}; \frac{3}{2}; -\Omega_2\right)$ and $\Theta_4 = {}_2F_1\left(\frac{1}{2}, m + \frac{3}{2}; \frac{3}{2}; -\Omega_2\right)$.

So the e2e SER, i.e., of the source-to-destination link via FD relay, for adaptive S-ER scheme SER_{e2e}^{adp} can be evaluated by substituting (86) and (91) in (17). This can be expressed as

$$SER_{e2e}^{adp} = SER_{SR} + SER_{RD} - SER_{SR}SER_{RD}. \tag{92}$$

B. FIXED S-ER SCHEME

In the fixed S-ER scheme, the antennas for information transmission are selected sequentially. The combined channel gain g is the sum of N_r^I independent Rayleigh fading channel gains. So, from [55], the distribution of resultant g is chi-square distribution with $2N_r^I$ degrees of freedom, which can be expressed as

$$f_G(g) = \frac{1}{(N_r^I - 1)!} e^{-g} g^{N_r^I - 1}. \tag{93}$$

1) SPECTRAL EFFICIENCY FOR FIXED S-ER SCHEME

Using (93), the ASE of the source-to-FD relay link as defined in (6) can be evaluated as

$$ASE_{SR} = \int_0^\infty \log_2\left(1 + \frac{g_1 P_s}{\sigma_{rsi}^2 + \sigma^2}\right) \frac{e^{-g_1} g_1^{N_r^I - 1}}{(N_r^I - 1)!} dg_1. \quad (94)$$

After some mathematical manipulations and using [52, Appendix A], (94) can be evaluated and the simplified closed-form expression for ASE of the source-to-FD relay link for the fixed S-ER scheme can be expressed as below:

$$ASE_{SR} = \frac{1}{\ln 2}\binom{N_r}{N_r^I}\exp\left(\frac{1}{A_1}\right)\sum_{k=0}^{N_r^I - 1} E_{k+1}\left(\frac{1}{A_1}\right), \quad (95)$$

where $A_1 = \frac{P_s}{\sigma_{rsi}^2 + \sigma^2}$.

Similarly, the ASE for FD relay-to-destination link for the fixed S-ER scheme can be evaluated from (8) utilizing (93),

$$ASE_{RD} = \int_0^\infty \log_2\left(1 + \frac{g_2 P_r}{\sigma^2}\right) \frac{e^{-g_2} g_2^{N_t^I - 1}}{(N_t^I - 1)!} dg_2,$$

$$= \frac{1}{\ln 2}\binom{N_t}{N_t^I}\exp\left(\frac{1}{A_2}\right)\sum_{k=0}^{N_t^I - 1} E_{k+1}\left(\frac{1}{A_2}\right), \quad (96)$$

where $A_2 = \frac{P_r}{\sigma^2}$.

The e2e ASE of the source-to-destination link for fixed S-ER scheme, ASE_{e2e}^{fix}, can now be expressed as

$$ASE_{e2e}^{fix} = \min\{ASE_{SR}, ASE_{RD}\}. \quad (97)$$

2) ENERGY EFFICIENCY FOR FIXED S-ER SCHEME

The AEE for fixed S-ER scheme as defined in (21) can now be evaluated utilizing (27), (28) and (97)

$$AEE_{e2e}^{fix}$$

$$= \frac{ASE_{e2e}^{fix}}{(1 + \beta)P_t + P_c^{FD} - \kappa(\eta_t N_t + \eta_r N_r)(1 - \eta_t)N_t P_R}. \quad (98)$$

3) OUTAGE FOR FIXED S-ER SCHEME

Now, P_{SR}^{out} and P_{RD}^{out} as defined in (13) and (16) respectively, can be evaluated for the fixed S-ER schemes as below:

Solving (13) by utilizing (93), the outage probabilities P_{SR}^{out} can be evaluated as

$$P_{SR}^{out} = \int_0^{z_1} \frac{1}{(N_r^I - 1)!} e^{-g_1} g_1^{N_r^I - 1} dg_1,$$

$$= 1 - \frac{\Gamma(N_r^I, z_1)}{\Gamma(N_r^I)}. \quad (99)$$

Similarly by utilizing (93) for solving (16), the outage probabilities P_{RD}^{out} can be evaluated as

$$P_{RD}^{out} = \int_0^{z_2} \frac{1}{(N_t^I - 1)!} e^{-g_2} g_2^{N_t^I - 1} dg_2,$$

$$= 1 - \frac{\Gamma(N_t^I, z_2)}{\Gamma(N_t^I)}. \quad (100)$$

Further, the e2e outage probability for the source-to-destination link via relay, P_{e2e} can be evaluated by substituting (99) and (100) in (10). After simplification the outage probability for fixed S-ER scheme, P_{e2e}^{fix} can be expressed as,

$$P_{e2e}^{fix} = P_{SR}^{out} + P_{RD}^{out} - P_{SR}^{out} P_{RD}^{out},$$

$$= 1 - \frac{\Gamma(N_r^I, z_1)}{\Gamma(N_r^I)} \frac{\Gamma(N_t^I, z_2)}{\Gamma(N_t^I)}. \quad (101)$$

From (101), it can be observed that as N_r^I or N_t^I increases, the overall outage probability decreases. Since N_r^I and N_t^I are inversely proportional to η_r and η_t respectively, hence that outage increases along with increasing η_r and η_t.

4) SYMBOL ERROR RATE FOR FIXED S-ER SCHEME

The SER for the source-to-FD relay link SER_{SR} as defined in (19) can be formulated by utilizing (69) and (93) as

$$SER_{SR} \approx \Upsilon \int_0^\infty \text{erfc}\left(\sqrt{\frac{3\rho(g_1)}{2(M-1)}}\right) f_G(g_1) dg_1,$$

$$= \Upsilon \int_0^\infty \text{erfc}\left(\sqrt{\Omega_1 g_1}\right) \frac{e^{-g_1} g_1^{N_r^I - 1}}{(N_r^I - 1)!} dg_1,$$

$$= \Upsilon\left[1 - \int_0^\infty \text{erf}\left(\sqrt{\Omega_1 g_1}\right) \frac{e^{-g_1} g_1^{N_r^I - 1}}{(N_r^I - 1)!} dg_1\right], \quad (102)$$

where $\Omega_1 = \frac{3P_s}{2(\sigma_{rsi}^2 + \sigma^2)(M-1)}$.

Substituting $\sqrt{\Omega_1} = \Lambda_1$, $\sqrt{g_1} = \chi_1$ the above expression can be reformulated as

$$SER_{SR} = \Upsilon\left[1 - 2\int_0^\infty \frac{\text{erf}(\Lambda_1 \chi_1) e^{-\chi_1^2} \chi_1^{2N_r^I - 1}}{(N_r^I - 1)!} d\chi_1\right]. \quad (103)$$

Using [54, eq. (4.3.8)], the closed expression for SER_{SR} in (103) can be evaluated as

$$SER_{SR} = \Upsilon\left[1 - \sqrt{\frac{\Omega_1}{\pi}} \frac{2\Gamma\left(N_r^I + \frac{1}{2}\right)}{(N_r^I - 1)!} \Theta_1\right], \quad (104)$$

where $\Theta_1 = {}_2F_1\left(\frac{1}{2}, N_r^I + \frac{1}{2}; \frac{3}{2}; -\Lambda_1^2\right)$.

Similarly the SER for the FD relay-to-destination link SER_{RD} as defined in (20) can be formulated as

$$SER_{RD} = \Upsilon\left[1 - \int_0^\infty \text{erf}\left(\sqrt{\Omega_2 g_2}\right) \frac{e^{-g_2} g_2^{N_t^I - 1}}{(N_t^I - 1)!} dg_2\right], \quad (105)$$

where $\Omega_2 = \frac{3P_r}{2(\sigma^2)(M-1)}$. Substituting $\sqrt{\Omega_2} = \Lambda_2$, $\sqrt{g_2} = \chi_2$ the above expression can be reformulated as

$$SER_{RD} = \Upsilon\left[1 - 2\int_0^\infty \frac{\text{erf}(\Lambda_2 \chi_2) e^{-\chi_2^2} \chi_2^{2N_t^I - 1}}{(N_t^I - 1)!} d\chi_2\right]. \quad (106)$$

Using [54, eq. (4.3.8)], the closed expression for SER_{RD} in (106) can be evaluated as

$$SER_{RD} = \Upsilon \left[1 - \sqrt{\frac{\Omega_2}{\pi}} \frac{2\Gamma\left(N_t^I + \frac{1}{2}\right)}{(N_t^I - 1)!} \Theta_2 \right], \quad (107)$$

where $\Theta_2 = {}_2F_1\left(\frac{1}{2}, N_t^I + \frac{1}{2}; \frac{3}{2}; -\Lambda_2^2\right)$.

Substituting (104) and (107) in (17), the e2e SER for fixed S-ER scheme SER_{e2e}^{fix} i.e., SER of the source-to-destination link via FD relay can be evaluated. This can be expressed as

$$SER_{e2e}^{fix} = SER_{SR}^{fix} + SER_{RD}^{fix} - SER_{SR}^{fix}SER_{RD}^{fix}. \quad (108)$$

IV. SIMULATION RESULTS

In this section, we show the ASE, outage, SER andd the AEE results for the FD-MIMO-DF relay system in the presence of proposed S-ER schemes. As discussed before, the channel assumed is flat Rayleigh fading. Further, the transmit power at the source and FD-relay is taken as $P_s = P_r = P_T$. Similarly, the circuit power consumption at the source, destination, SIC circuit and the relay is assumed to be P_c, i.e., $P_c^S = P_c^R = P_c^D = P_{co} = P_c$. The remaining simulation parameters are listed in Table 1.

TABLE 1. Simulation parameters.

Parameter	Simulation Values
Antennas at the FD Relay	$N_t=10\ N_r=10$
Rate Threshold	$R_{th} = 3$ bps/Hz
RF-to-DC conversion efficiency	$\kappa = 0.5$
Variance of AWGN Noise	$\sigma^2 = 0$ dB
Variance of channel elements	1
RSI parameter	$\nu =1\ , \alpha = 0.01$
Co-efficient for HPA Power Consumption Model	$\beta = 0.8$

A. SE AND EE RESULTS

Fig. 4 shows the ASE of the source-to-FD relay link, FD relay-to-destination and source-to-destination link via the FD relay. From the result, it can be observed that the ASE of the e2e source-to-destination link primarily depends on the source-to-FD relay link. For instance, at $P_T = 20$ dB, the ASE of source-to-FD relay link is 9 bps/Hz, whereas for the FD relay-to-destination link ASE is 10 bps/Hz and the source-to-destination link is also 9 bps. This is due to the fact that the source-to-FD relay link is impacted by the SI, and the FD relay-to-destination link is free from interference. Thus, the antennas at the transmit side of the FD relay can be employed for S-ER.

Fig. 5 shows the impact of S-ER on ASE and AEE for $\eta_r = 0$, $\eta_t = 0.3$ and $P_c = 0$. The results show that the adaptive S-ER scheme provides the best AEE compared to fixed S-ER and without S-ER. Further, $\eta_t = 0.3$ implies that $N_t^I = 7$ antennas are utilized for information transmission, and the remaining 3 antennas are used for S-ER at the transmit end of the FD relay, whereas $\eta_r = 0$ implies that all the antennas are used for information reception at the receiving end
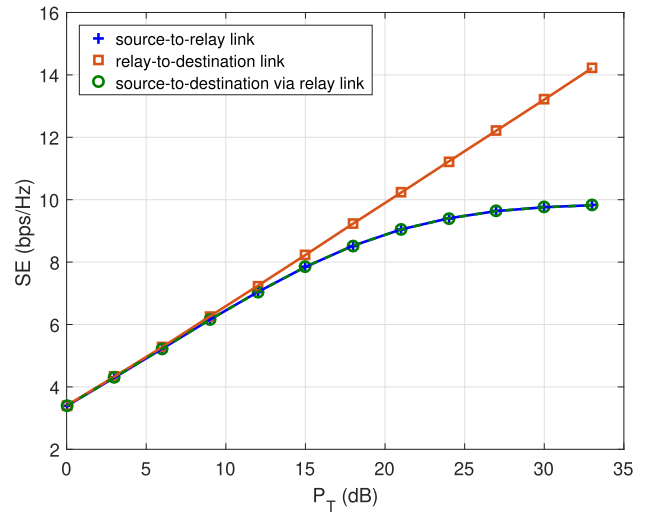

FIGURE 4. Analytical (solid lines) and simulation (marker points) shows the SE for the source-to-FD relay, relay-to-destination and source-to-destination link various distinct transmit power level.

of the FD relay. As discussed earlier, the e2e ASE primarily depends on the source-to-FD relay link. Thus, nearly the same ASE can be observed with and without S-ER, as evident from Fig. 5(a), specifically the ASE for adaptive S-ER is almost equivalent to the ASE without S-ER. However, there is a considerable gain in AEE, for instance, as shown in Fig. 5(b), the AEE at $P_T = 10$ dB is 0.3 bits/Hz/Joule without S-ER, whereas with S-ER it increases to 0.6 bits/Hz/Joule.

Fig. 6 shows the ASE and AEE for $\eta_r = 0.3$, $\eta_t = 0.3$, which implies that S-ER is employed at both transmit and receive end of relay. As discussed before, this will lead to a reduction in the antenna array gain of the source-to-FD relay link, and hence, there would be a slight degradation in SE, as shown in Fig. 6(a). However, by utilizing the adaptive S-ER scheme, the loss due to antenna array gain can be compensated, as shown through the results. Fig. 6 also validates that adaptive S-ER not only provides nearly equal ASE vis-a-vis full antenna transmission but also contributes to the AEE compared to the case without S-ER. For instance, in Fig. 6(a), at $P_T = 15$ dB the ASE without S-ER is 7.8 bps/Hz, however with a fixed S-ER scheme, the ASE reduces to 7.2 bps/Hz. The degradation in ASE can somewhat be compensated through adaptive S-ER scheme, which results in ASE of 7.7 bps/Hz, nearly equal to the ASE of without S-ER case. Similarly, from Fig. 6(b) the AEE at $P_T = 10$ dB for without S-ER case is 0.3 bit/Hz/Joule, whereas with S-ER AEE increases significantly to 1 bit/Hz/Joule. The results confirm that the adaptive S-ER scheme provides the best performance in terms of AEE, while also providing the ASE which is nearly equivalent to the case of without S-ER.

B. IMPACT OF CIRCUIT POWER ON EE

Fig. 7 shows the impact of circuit power on the AEE of a FD-MIMO-DF relay system for $\eta = 0.3$.
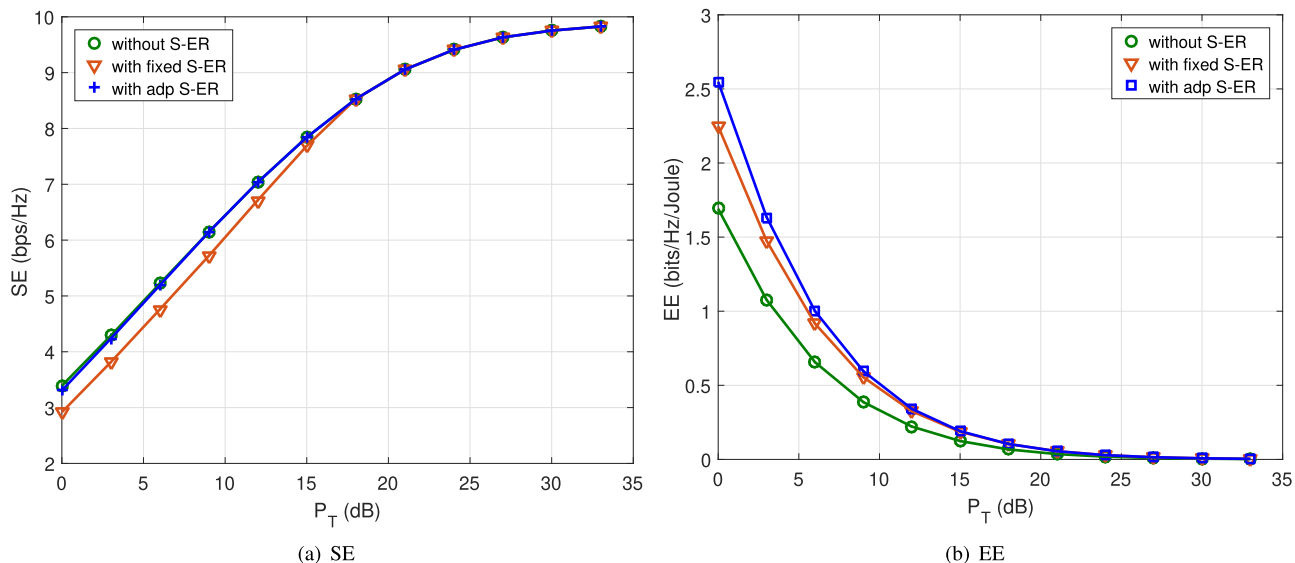
(a) SE

(b) EE

FIGURE 5. Analytical (solid lines) and simulation (marker points) results of SE and EE with respect to P_T for various S-ER cases at $\eta_r = 0$, $\eta_t = 0.3$ and $P_c = 0$.
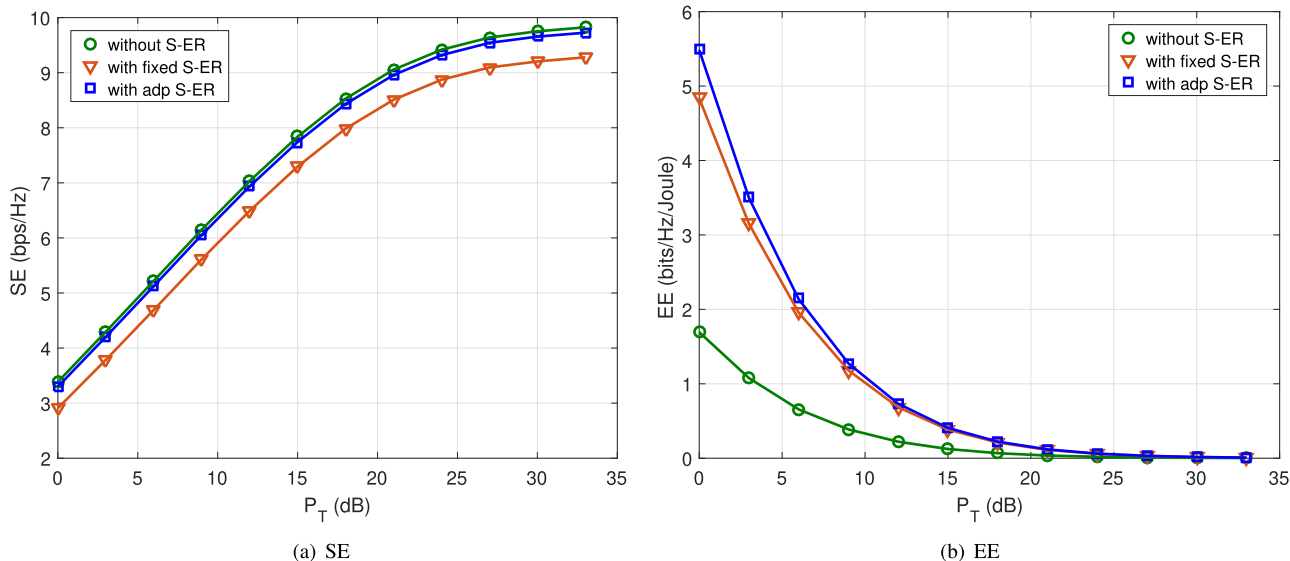

(a) SE

(b) EE

FIGURE 6. Analytical (solid lines) and simulation (marker points) results of SE and EE with respect to P_T for various S-ER cases at $\eta_r = 0.3$, $\eta_t = 0.3$ and $P_c = 0$.

Fig. 7(a) and 7(b) shows the AEE of various S-ER schemes at $P_c = 3$ dB and $P_c = 10$ dB respectively. It can be observed from Fig. 7(b) that at $P_T = 10$ dB, the AEE without S-ER is 0.10 bits/Hz/Joule, whereas with S-ER it increases to 0.13 bits/Hz/Joule for fixed S-ER scheme and 0.14 bits/Hz/Joule for adaptive S-ER scheme. This improvement in AEE is also due to the fact that in the case of adaptive S-ER, there is a reduction in circuit power consumption as the number of active RF chains are reduced, and the antennas corresponding to the inactive RF chains are being utilized for S-ER. It can be observed that initially, AEE increases and then decreases with P_T. This is due to the fact that P_T increases

exponentially whereas the SE increases linearly with respect to the P_T, thus when P_T is small, AEE increases due to increase in ASE, whereas for larger values the exponential increase of P_T dominates, and hence AEE decreases again. This can be also be observed from (21). It is obvious from Fig. 7 that, for $P_c = 3$ dB the maximum AEE is at $P_T = 9$ dB, whereas when the circuit power is increased to $P_c = 10$ dB the maximum AEE shifts between 12 to 15 dB of P_T.

C. TRADE-OFF BETWEEN THE EE AND SE

The trade-off between the EE and the SE in context of the proposed S-ER scheme is shown in Fig. 8. It can be observed
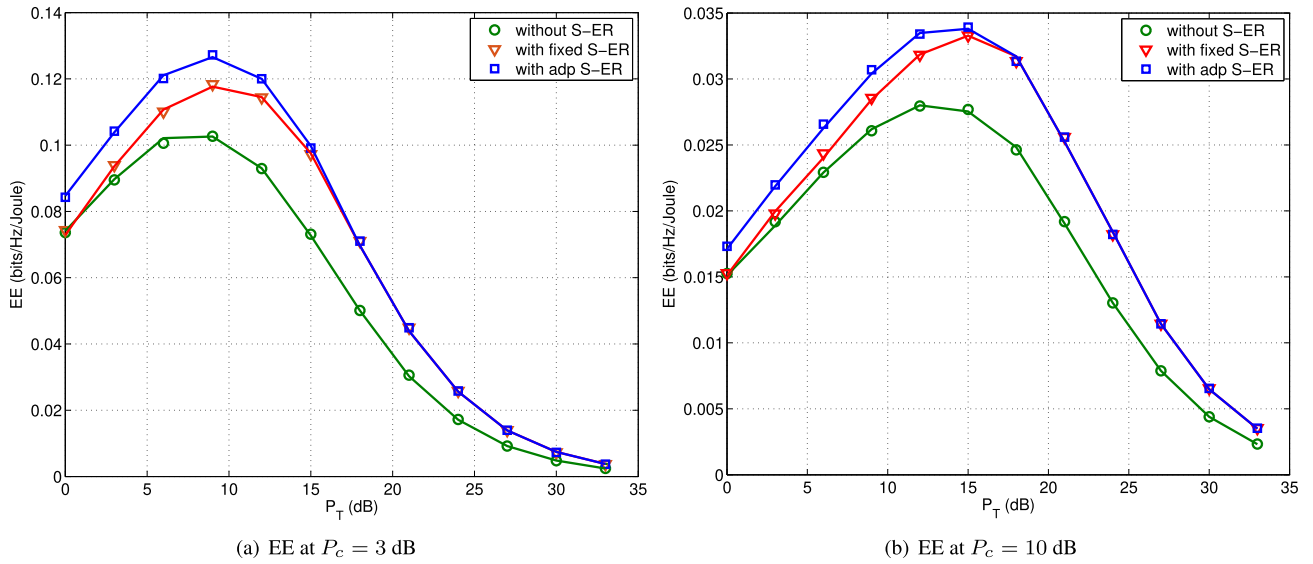
(a) EE at $P_c = 3$ dB

(b) EE at $P_c = 10$ dB

FIGURE 7. Analytical (solid lines) and simulation (marker points) results of EE with respect to P_T for various S-ER cases at $\eta = 0.3$ and different P_c.

(a) EE versus SE without P_c

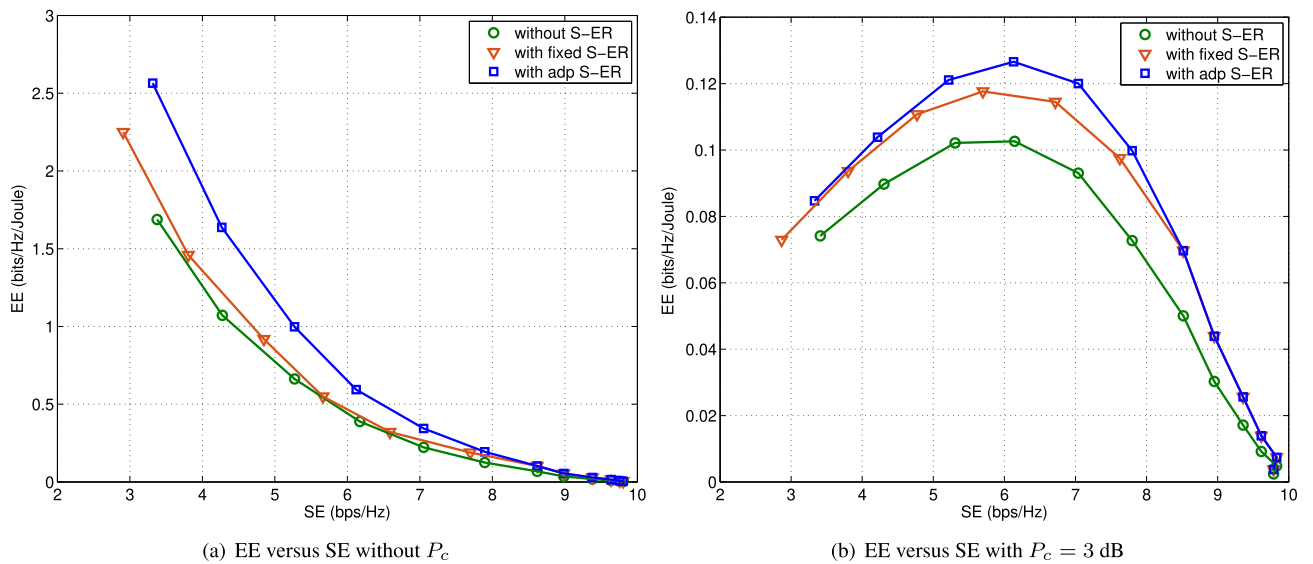(b) EE versus SE with $P_c = 3$ dB

FIGURE 8. Analytical (solid lines) and simulation (marker points) shows the trade-off between the SE and the EE with respect to antenna allocation for both the S-ER schemes at $\eta = 0.3$ and different P_c.

from the results that increasing the SE reduces the EE of the FD-relay system. However, for a fixed SE, the adaptive S-ER scheme provides the best EE. Specifically, Fig. 8(a) shows the performance trade-off of the FD relay system between the EE and SE without considering the impact of circuit power. As evident from the result, the adaptive S-ER scheme provides the best EE for a any given SE. Further, it can also be observed that increasing the SE reduces the EE whereas the most energy efficient region is the one corresponding to the least SE.

The impact of circuit power on the trade-off of the EE with the SE can be seen in Fig. 8(b). It can be observed from the result that the most energy efficient region is not the one

corresponding to the least SE, however, the maximum EE is obtained at the SE of around 6 bps/Hz, whereas further increase in SE leads to the reduction in the EE of the FD-relay system. Moreover, the adaptive S-ER scheme provides the best EE for any given SE, which is consistent with the earlier observations.

D. OUTAGE PERFORMANCE

Fig. 9 shows that the outage performance for both fixed S-ER and adaptive S-ER schemes. The analytical results are in good agreement with the simulation results, which validates the closed-form expressions obtained in the paper. It can be
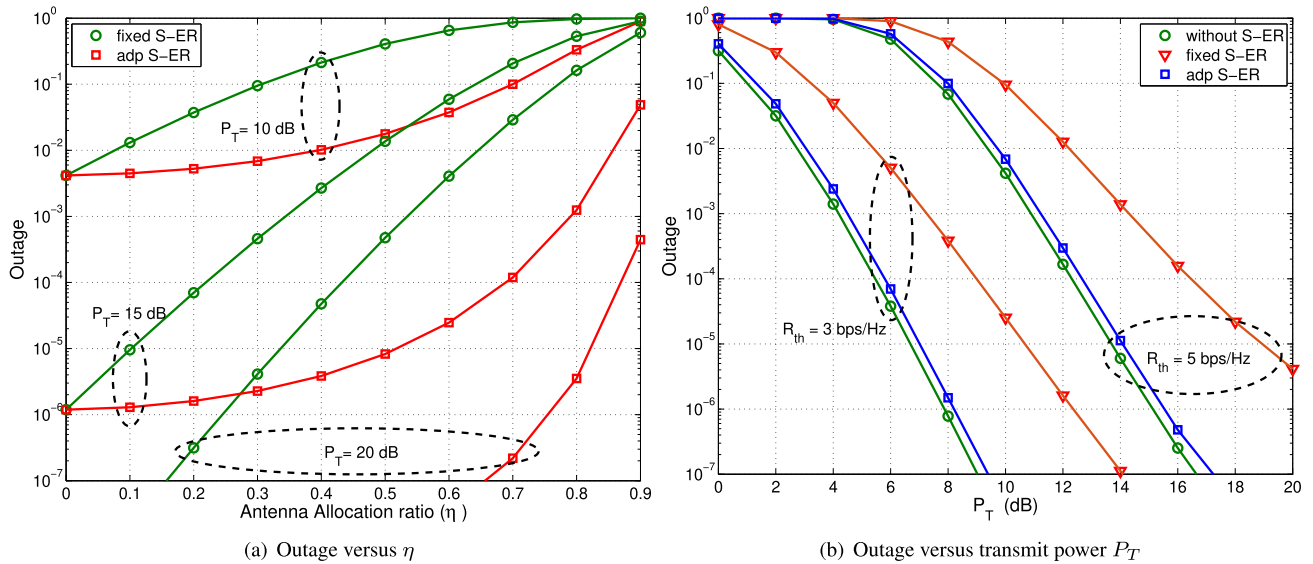
(a) Outage versus η

(b) Outage versus transmit power P_T

FIGURE 9. Analytical (solid lines) and simulation (marker points) shows the outage performance with respect to η and various distinct transmit power level for both the two S-ER schemes.

observed from Fig. 9(a), that the outage increases with η. This is due to the fact that increasing η implies that N_{S-ER} increases and subsequently N_I decreases, which lowers the diversity gain, consequently increasing the outage. Fig. 9(a) also shows that the outage performance for the adaptive S-ER scheme outperforms the fixed S-ER scheme. For instance, at $\eta = 0.5$ the outage probability for $P_T = 15$dB is 10^{-5} for adaptive S-ER scheme, whereas for fixed S-ER scheme it is 10^{-2}. Further, it can also be observed that for $P_T = 15$ dB, the outage probability for the case of without S-ER, i.e., $\eta = 0$ is 10^{-6} which is quite closer that can be achieved by adaptive S-ER scheme. Thus, as evident from the results the adaptive S-ER scheme compensate for the loss in performance that is observed in the fixed S-ER scheme. Since in the adaptive S-ER, adaptive antenna allocation based on channel gain provides additional diversity gain for the same number of antennas as compared to fixed antenna allocation, hence, the adaptive S-ER scheme performs considerably better than the fixed S-ER scheme.

Fig. 9(b) shows the outage probability with respect to transmit power. It can be observed from the result that S-ER increases the outage probability. However, in the adaptive S-ER scheme, the degradation in outage performance is somewhat compensated. For instance, at $P_T = 6$ dB for $R_{th} = 3$ bps/Hz the outage probability for without S-ER case is 3×10^{-5} and for the fixed S-ER the outage increases to 4×10^{-3}. However, the adaptive S-ER scheme nearly compensates for the degradation in the outage. Specifically, the outage probability for adaptive S-ER for the same parameters is 5×10^{-5}. Further, it can also be observed that the outage increases when the rate threshold R_{th} increases. Thus as evident from the results, the adaptive S-ER provides nearly the same outage performance as without S-ER case. Thus,

the adaptive S-ER technique not only enhances the EE but also maintains the outage performance.

E. SER PERFORMANCE

Fig. 10 shows the SER performance for both fixed S-ER and adaptive S-ER schemes. The results show that adaptive S-ER performs far better than the fixed S-ER in terms of SER. Specifically, Fig. 10(a) shows the SER performance with respect to the antenna allocation ratio η. It can also be observed that increasing η increase the error rate which is quite obvious as increasing η implies that more number of antennas are harvesting energy and less number of antennas are available for information relaying. Further, it also shows that the proposed adaptive S-ER utilizes the channel gain opportunistically. For instance, it can be observed from Fig. 10(a), that SER at $\eta = 0.3$ and $P_T = 10$ dB is around 10^{-3} for adaptive S-ER, whereas for fixed S-ER the corresponding SER is around 10^{-2}. It can also be seen that for the case of without S-ER, i.e., $\eta = 0$ the SER is 10^{-3}, which can nearly be achieved with adaptive S-ER for smaller values of η. Thus, in the adaptive S-ER, the EE is increased while maintaining the required SER and outage performance.

Fig. 10(b) shows the SER performance of adaptive S-ER, fixed S-ER and without S-ER schemes with respect to transmit power for $M = 16$ and $M = 64$. It can easily be observed from the result that the proposed adaptive S-ER scheme has nearly the same SER performance as that of without S-ER case. Further, it also shows that increasing the modulation level increases SER. Hence, it can be concluded from Fig. (9) and Fig. (10), that the proposed adaptive S-ER scheme enhances the energy efficiency while maintaining the desired quality-of-service (QoS) requirement, as shown in terms of outage and SER performance, respectively.
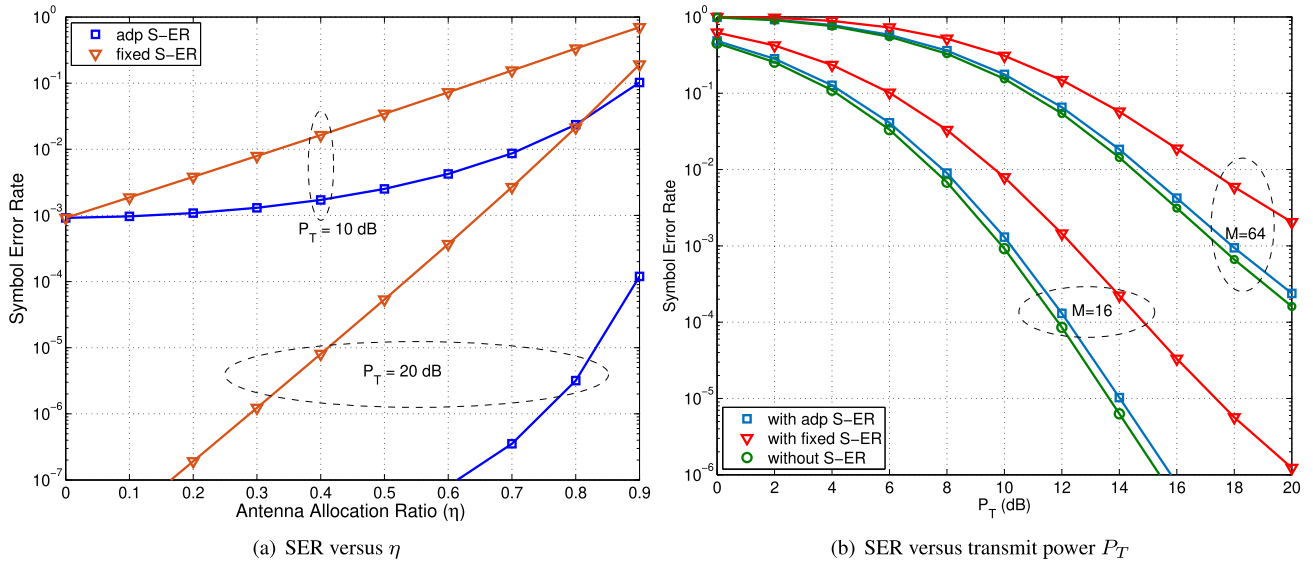
(a) SER versus η

(b) SER versus transmit power P_T

FIGURE 10. Analytical (solid lines) and simulation (marker points) results of SER with respect to antenna allocation ratio η and various S-ER cases at different transmit power level.

V. CONCLUSION

In this work, the impact of S-ER on the SE, outage, SER and the EE of a FD-MIMO-DF relaying system is investigated. Two S-ER schemes, namely fixed S-ER scheme and adaptive S-ER scheme, are proposed and analyzed. The closed-form expressions for outage performance, SER, ASE and EE are also derived for the proposed S-ER schemes. It has been shown that as the number of antennas for S-ER at the FD relay increases, there is a corresponding gain in the EE due to recycling a part of transmitted signal power. However, this results in a reduction in array gain and leads to a slight degradation in the ASE, SER and outage performance. Further, we have shown that via the proposed adaptive S-ER scheme, the degradation in ASE, SER and outage can be compensated while increasing the EE. The results also confirm that the adaptive S-ER scheme enhances the EE while maintaining the ASE, SER and the outage. Along with the analytical expressions, simulation results were also presented to verify the efficacy of the proposed analytical framework.

REFERENCES

[1] M. A. Habibi, M. Nasimi, B. Han, and H. D. Schotten, "A comprehensive survey of RAN architectures toward 5G mobile communication system," *IEEE Access*, vol. 7, pp. 70371–70421, May 2019.

[2] M. P. Mills, "The cloud begins with coal," Digital Power Group, Tech. Rep., 2013.

[3] M. Shafi, A. F. Molisch, P. J. Smith, T. Haustein, P. Zhu, P. De Silva, F. Tufvesson, A. Benjebbour, and G. Wunder, "5G: A tutorial overview of standards, trials, challenges, deployment, and practice," *IEEE J. Sel. Areas Commun.*, vol. 35, no. 6, pp. 1201–1221, Jun. 2017.

[4] A. Fehske, G. Fettweis, J. Malmodin, and G. Biczok, "The global footprint of mobile communications: The ecological and economic perspective," *IEEE Commun. Mag.*, vol. 49, no. 8, pp. 55–62, Aug. 2011.

[5] P. Mertikopoulos and E. V. Belmega, "Learning to be green: Robust energy efficiency maximization in dynamic MIMO–OFDM systems," *IEEE J. Sel. Areas Commun.*, vol. 34, no. 4, pp. 743–757, Apr. 2016.

[6] P. Skillermark and P. Frenger, "Enhancing energy efficiency in LTE with antenna muting," in *Proc. IEEE 75th Veh. Technol. Conf. (VTC Spring)*, May 2012, pp. 1–5.

[7] Z. Niu, Y. Wu, J. Gong, and Z. Yang, "Cell zooming for cost-efficient green cellular networks," *IEEE Commun. Mag.*, vol. 48, no. 11, pp. 74–79, Nov. 2010.

[8] S. Kim, R. Vyas, J. Bito, K. Niotaki, A. Collado, A. Georgiadis, and M. M. Tentzeris, "Ambient RF energy-harvesting technologies for self-sustainable standalone wireless sensor platforms," *Proc. IEEE*, vol. 102, no. 11, pp. 1649–1666, Nov. 2014.

[9] G. Piro, M. Miozzo, G. Forte, N. Baldo, L. A. Grieco, G. Boggia, and P. Dini, "HetNets powered by renewable energy sources: Sustainable next-generation cellular networks," *IEEE Internet Comput.*, vol. 17, no. 1, pp. 32–39, Jan. 2013.

[10] X. Lu, P. Wang, D. Niyato, D. I. Kim, and Z. Han, "Wireless networks with RF energy harvesting: A contemporary survey," *IEEE Commun. Surveys Tuts.*, vol. 17, no. 2, pp. 757–789, 2nd Quart., 2015.

[11] Y. Mao, Y. Luo, J. Zhang, and K. B. Letaief, "Energy harvesting small cell networks: Feasibility, deployment, and operation," *IEEE Commun. Mag.*, vol. 53, no. 6, pp. 94–101, Jun. 2015.

[12] S. Ulukus, A. Yener, E. Erkip, O. Simeone, M. Zorzi, P. Grover, and K. Huang, "Energy harvesting wireless communications: A review of recent advances," *IEEE J. Sel. Areas Commun.*, vol. 33, no. 3, pp. 360–381, Mar. 2015.

[13] R. Mahapatra, Y. Nijsure, G. Kaddoum, N. Ul Hassan, and C. Yuen, "Energy efficiency tradeoff mechanism towards wireless green communication: A survey," *IEEE Commun. Surveys Tuts.*, vol. 18, no. 1, pp. 686–705, 1st Quart., 2016.

[14] S. Buzzi, C.-L. I, T. E. Klein, H. V. Poor, C. Yang, and A. Zappone, "A survey of energy-efficient techniques for 5G networks and challenges ahead," *IEEE J. Sel. Areas Commun.*, vol. 34, no. 4, pp. 697–709, Apr. 2016.

[15] P. Gandotra, R. K. Jha, and S. Jain, "Green communication in next generation cellular networks: A survey," *IEEE Access*, vol. 5, pp. 11727–11758, Jul. 2017.

[16] Q. Wu, G. Y. Li, W. Chen, D. W. K. Ng, and R. Schober, "An overview of sustainable green 5G networks," *IEEE Wireless Commun.*, vol. 24, no. 4, pp. 72–80, Aug. 2017.

[17] G. Liu, F. R. Yu, H. Ji, V. C. M. Leung, and X. Li, "In-band full-duplex relaying: A survey, research issues and challenges," *IEEE Commun. Surveys Tuts.*, vol. 17, no. 2, pp. 500–524, 2nd Quart., 2015.

[18] S. Li, K. Yang, M. Zhou, J. Wu, L. Song, Y. Li, and H. Li, "Full-duplex amplify-and-forward relaying: Power and location optimization," *IEEE Trans. Veh. Technol.*, vol. 66, no. 9, pp. 8458–8468, Sep. 2017.

[19] B. Yu, L. Yang, X. Cheng, and R. Cao, "Power and location optimization for full-duplex Decode-and-Forward relaying," *IEEE Trans. Commun.*, vol. 63, no. 12, pp. 4743–4753, Dec. 2015.

[20] H. Cui, M. Ma, L. Song, and B. Jiao, "Relay selection for two-way full duplex relay networks with Amplify-and-Forward protocol," *IEEE Trans. Wireless Commun.*, vol. 13, no. 7, pp. 3768–3777, Jul. 2014.

[21] T. K. Baranwal, D. S. Michalopoulos, and R. Schober, "Outage analysis of multihop full duplex relaying," *IEEE Commun. Lett.*, vol. 17, no. 1, pp. 63–66, Jan. 2013.

[22] Z. Zhang, Z. Ma, M. Xiao, G. K. Karagiannidis, Z. Ding, and P. Fan, "Two-timeslot two-way full-duplex relaying for 5G wireless communication networks," *IEEE Trans. Commun.*, vol. 64, no. 7, pp. 2873–2887, Jul. 2016.

[23] Z. Zhang, X. Chai, K. Long, A. V. Vasilakos, and L. Hanzo, "Full duplex techniques for 5G networks: Self-interference cancellation, protocol design, and relay selection," *IEEE Commun. Mag.*, vol. 53, no. 5, pp. 128–137, May 2015.

[24] M. Heino, D. Korpi, T. Huusari, E. Antonio-Rodriguez, S. Venkatasubramanian, T. Riihonen, L. Anttila, C. Icheln, K. Haneda, R. Wichman, and M. Valkama, "Recent advances in antenna design and interference cancellation algorithms for in-band full duplex relays," *IEEE Commun. Mag.*, vol. 53, no. 5, pp. 91–101, May 2015.

[25] E. Ahmed, A. M. Eltawil, and A. Sabharwal, "Self-interference cancellation with nonlinear distortion suppression for full-duplex systems," in *Proc. Asilomar Conf. Signals, Syst. Comput.*, Nov. 2013, pp. 1199–1203.

[26] T. Riihonen, S. Werner, and R. Wichman, "Mitigation of loopback self-interference in full-duplex MIMO relays," *IEEE Trans. Signal Process.*, vol. 59, no. 12, pp. 5983–5993, Dec. 2011.

[27] C. Xing, S. Ma, and Y.-C. Wu, "Robust joint design of linear relay precoder and destination equalizer for dual-hop amplify-and-forward MIMO relay systems," *IEEE Trans. Signal Process.*, vol. 58, no. 4, pp. 2273–2283, Apr. 2010.

[28] A. Almradi and K. A. Hamdi, "MIMO full-duplex relaying in the presence of co-channel interference," *IEEE Trans. Veh. Technol.*, vol. 66, no. 6, pp. 4874–4885, Jun. 2017.

[29] X. Xia, K. Xu, Y. Wang, and Y. Xu, "A 5G-enabling technology: Benefits, feasibility, and limitations of in-band full-duplex mMIMO," *IEEE Veh. Technol. Mag.*, vol. 13, no. 3, pp. 81–90, Sep. 2018.

[30] L. Jiménez Rodríguez, N. H. Tran, and T. Le-Ngoc, "Performance of full-duplex AF relaying in the presence of residual self-interference," *IEEE J. Sel. Areas Commun.*, vol. 32, no. 9, pp. 1752–1764, Sep. 2014.

[31] L. Jimenez Rodriguez, N. H. Tran, and T. Le-Ngoc, "Optimal power allocation and capacity of full-duplex AF relaying under residual self-interference," *IEEE Wireless Commun. Lett.*, vol. 3, no. 2, pp. 233–236, Apr. 2014.

[32] Y. Zeng and R. Zhang, "Full-duplex wireless-powered relay with self-energy recycling," *IEEE Wireless Commun. Lett.*, vol. 4, no. 2, pp. 201–204, Apr. 2015.

[33] D. Hwang, K. Cheol Hwang, D. In Kim, and T.-J. Lee, "Self-energy recycling for RF powered multi-antenna relay channels," *IEEE Trans. Wireless Commun.*, vol. 16, no. 2, pp. 812–824, Feb. 2017.

[34] A. Yadav, O. A. Dobre, and H. V. Poor, "Is self-interference in full-duplex communications a foe or a friend?" *IEEE Signal Process. Lett.*, vol. 25, no. 7, pp. 951–955, Jul. 2018.

[35] Ö. T. Demir and T. E. Tuncer, "Optimum QoS-aware beamformer design for full-duplex relay with self-energy recycling," *IEEE Wireless Commun. Lett.*, vol. 7, no. 1, pp. 122–125, Feb. 2018.

[36] D. Hwang, S. S. Nam, and J. Yang, "Multi-antenna beamforming techniques in full-duplex and self-energy recycling systems: Opportunities and challenges," *IEEE Commun. Mag.*, vol. 55, no. 10, pp. 160–167, Oct. 2017.

[37] P. Grover and A. Sahai, "Shannon meets tesla: Wireless information and power transfer," in *Proc. IEEE Int. Symp. Inf. Theory*, Jun. 2010, pp. 2363–2367.

[38] Z. Ding, C. Zhong, D. Wing Kwan Ng, M. Peng, H. A. Suraweera, R. Schober, and H. V. Poor, "Application of smart antenna technologies in simultaneous wireless information and power transfer," *IEEE Commun. Mag.*, vol. 53, no. 4, pp. 86–93, Apr. 2015.

[39] M. Mohammadi, B. K. Chalise, H. A. Suraweera, C. Zhong, G. Zheng, and I. Krikidis, "Throughput analysis and optimization of wireless-powered multiple antenna full-duplex relay systems," *IEEE Trans. Commun.*, vol. 64, no. 4, pp. 1769–1785, Apr. 2016.

[40] H. Liang, C. Zhong, X. Chen, H. A. Suraweera, and Z. Zhang, "Wireless powered dual-hop multi-antenna relaying systems: Impact of CSI and antenna correlation," *IEEE Trans. Wireless Commun.*, vol. 16, no. 4, pp. 2505–2519, Apr. 2017.

[41] C. Zhong, H. A. Suraweera, G. Zheng, I. Krikidis, and Z. Zhang, "Wireless information and power transfer with full duplex relaying," *IEEE Trans. Commun.*, vol. 62, no. 10, pp. 3447–3461, Oct. 2014.

[42] H. Chen, G. Li, and J. Cai, "Spectral–energy efficiency tradeoff in full-duplex two-way relay networks," *IEEE Syst. J.*, vol. 12, no. 1, pp. 583–592, Mar. 2018.

[43] C. Li, Z. Chen, Y. Wang, Y. Yao, and B. Xia, "Outage analysis of the full-duplex decode-and-forward two-way relay system," *IEEE Trans. Veh. Technol.*, vol. 66, no. 5, pp. 4073–4086, May 2017.

[44] L. V. Nguyen, B. C. Nguyen, X. N. Tran, and L. T. Dung, "Closed-form expression for the symbol error probability in full-duplex spatial modulation relay system and its application in optimal power allocation," *Sensors*, vol. 19, no. 24, p. 5390, Dec. 2019.

[45] J. G. Proakis and M. Salehi, *Digital Communications*, 5th ed. New York, NY, USA: McGraw-Hill, 2007.

[46] I. S. Gradshteyn and I. M. Ryzhik, *Table of Integrals, Series, and Products*, 7th ed. Boston, MA, USA: Elsevier, 2014.

[47] H. Li, L. Song, and M. Debbah, "Energy efficiency of large-scale multiple antenna systems with transmit antenna selection," *IEEE Trans. Commun.*, vol. 62, no. 2, pp. 638–647, Feb. 2014.

[48] J. Ma and C. Huang, "Energy efficiency of decode-and-forward full-duplex relay channels," in *Proc. IEEE Global Commun. Conf. (GLOBECOM)*, Dec. 2018, pp. 1–6.

[49] J. Qiao, H. Zhang, F. Zhao, and D. Yuan, "Secure transmission and self-energy recycling with partial eavesdropper CSI," *IEEE J. Sel. Areas Commun.*, vol. 36, no. 7, pp. 1531–1543, Jul. 2018.

[50] M. R. A. Khandaker and K.-K. Wong, "Robust secrecy beamforming with energy-harvesting eavesdroppers," *IEEE Wireless Commun. Lett.*, vol. 4, no. 1, pp. 10–13, Feb. 2015.

[51] H.-C. Yang and M.-S. Alouini, *Order Statistics in Wireless Communications: Diversity, Adaptation, and Scheduling in MIMO and OFDM Systems*. Cambridge, U.K.: Cambridge Univ. Press, 2011.

[52] H. Shin and J. Hong Lee, "Capacity of multiple-antenna fading channels: Spatial fading correlation, double scattering, and keyhole," *IEEE Trans. Inf. Theory*, vol. 49, no. 10, pp. 2636–2647, Oct. 2003.

[53] P. Aggarwal and V. A. Bohara, "End-to-end theoretical evaluation of a nonlinear MIMO-OFDM system in the presence of digital predistorter," *IEEE Syst. J.*, vol. 13, no. 3, pp. 2309–2319, Sep. 2019.

[54] W. N. Edward and M. Geller, "A table of integrals of the error functions," *J. Res. Nat. Bur. Stand.*, vol. 73B, no. 1, pp. 1–20, Oct. 1968.

[55] M. K. Simon and M.-S. Alouini, *Digital Communication Over Fading Channels*. New York, NY, USA: Wiley, 2005.

MOHD HAMZA NAIM SHAIKH (Member, IEEE) received the B.Tech. and M.Tech. degrees from Aligarh Muslim University, Aligarh, India, in 2014 and 2016, respectively. He is currently pursuing the Ph.D. degree with IIIT-Delhi, New Delhi, India. His research interests include next-generation communication technologies, such as full-duplex, massive MIMO, and energy-efficient wireless system design.

VIVEK ASHOK BOHARA (Senior Member, IEEE) received the Ph.D. degree from the School of Electrical and Electronic Engineering (EEE), Nanyang Technological University (NTU), Singapore, in 2011. From 2011 to 2013, he was a Postdoctoral Researcher (Marie Curie Fellowship) with the ESIEE Paris, University Paris-East. He joined IIIT-Delhi in 2013, where he is currently working as an Associate Professor. His research interests include towards next-generation communication technologies, such as device-to-device communication, carrier aggregation, and digital predistortion algorithms. He received 1st Prize in National Instruments ASEAN Virtual Instrumentation Applications Contest in 2007 and 2010. He was a recipient of Best Poster Award at IEEE ANTS 2014 and IEEE COMSNETS 2015 and 2016 conferences.

ANAND SRIVASTAVA (Member, IEEE) received the M.Tech. and Ph.D. degrees from the Indian Institute of Technology (IIT) Delhi, India, in 2002. Before joining IIIT-Delhi in 2014, he was the Dean and a Professor with the School of Computing and Electrical Engineering, IIT Mandi, India, from 2012 to 2014. He has been an Adjunct Professor with IIT Delhi since 2008. Prior to this, he worked with Alcatel-Lucent-Bell Labs, India, from 2009 to 2012, and the Center for Development of Telematics (CDOT), and a Telecom Research Center of Government of India from 1989 to 2008. During his stint in CDOT for nearly two decades, he was responsible for the development of national-level projects for Indian Telecom in the areas of telecom security systems, network management systems, intelligent networks, operations support systems, access networks (GPON), and optical technology based products. Majority of these projects were completed successfully and commercially deployed in the public network. He also carried out significant research work in the Photonics Research Laboratory, Nice, France, under the Indo-French Science and Technology Cooperation Program on Special optical fibers and fiber-based components for optical communications from 2007 to 2010. He was also closely involved with ITU-T, Geneva in Study Group 15 and represented India for various optical networking standards meetings. He has published several articles in peer-reviewed journals and conferences. He has visited Aston University, U.K., four times from 2014 to 2016 as a Visiting Scholar under Erasmus Mundus EU program for carrying out research in optical wireless area. His current research interests include optical core and access networks, fiber-wireless (FiWi) architectures, visible light communications (VLC), optical signal processing, free space optical communications, and energy aware optical networks.

● ● ●